Received: 12 January 2022 | Revised: 17 May 2022 | Accepted: 17 May 2022

DOI: 10.1002/glia.24224

GLIA

WILEY

REVIEW ARTICLE

Honey, I shrunk the extracellular space: Measurements and mechanisms of astrocyte swelling

Erin Walch[1] | Todd A. Fiacco[2,3]

[1]Division of Biomedical Sciences, School of Medicine, University of California, Riverside, Riverside, California, USA

[2]Department of Molecular, Cell and Systems Biology, University of California, Riverside, Riverside, California, USA

[3]Center for Glial-Neuronal Interactions, University of California, Riverside, Riverside, California, USA

Correspondence
Todd A. Fiacco, University of California, Riverside, 3401 Watkins Dr., 1229 Spieth Hall, Riverside, CA 92521, USA.
Email: toddf@ucr.edu

Funding information
Center for Scientific Review, Grant/Award Numbers: DA048815-01, NS109918-01; UCR Academic Senate; NIH NIDA; NIH NINDS

Abstract

Astrocyte volume fluctuation is a physiological phenomenon tied closely to the activation of neural circuits. Identification of underlying mechanisms has been challenging due in part to use of a wide range of experimental approaches that vary between research groups. Here, we first review the many methods that have been used to measure astrocyte volume changes directly or indirectly. While the field has recently shifted towards volume analysis using fluorescence microscopy to record cell volume changes directly, established metrics corresponding to extracellular space dynamics have also yielded valuable insights. We then turn to analysis of mechanisms of astrocyte swelling derived from many studies, with a focus on volume changes tied to increases in extracellular potassium concentration ($[K^+]_o$). The diverse methods that have been utilized to generate the external $[K^+]_o$ environment highlight multiple scenarios of astrocyte swelling mediated by different mechanisms. Classical potassium buffering theories are tempered by many recent studies that point to different swelling pathways optimized at particular $[K^+]_o$ and that depend on local/transient versus more sustained increases in $[K^+]_o$.

KEYWORDS
AQP4, ATPase, buffering, ECS, potassium, pump, volume, water

1 | INTRODUCTION

A little over 30 years ago, R.K. Orkand wrote: "the observations delineating glial membrane properties and processes that have given us a physiological basis for glial function have been made in a variety of model systems under admittedly unphysiological conditions" (Ballanyi et al., 1987). Since then, and despite progress made in imaging systems, transgenic lines, and in vivo models, the field has struggled to understand brain cell swelling and how best to measure it. Direct measurements are surprisingly lacking and therefore cell volume fluctuations have been inferred from measurements of the brain interstitial space in many instances. Knowledge of ion channels, pumps, and transporters expressed by astrocytes has steadily grown, but understanding their roles in cell volume changes have proven difficult and controversial. Information about how water itself crosses astrocyte membranes is also limited and often not addressed in most studies. This likely stems from limitations in methods used to quantify cell volume and the many ways in which cell swelling has been modeled experimentally. In an effort to understand these divergences, we will provide a critical analysis of the methodologies along with a summary model of proposed mechanisms underlying astrocyte swelling.

1.1 | Cell swelling: What is it and why is it important?

Cell swelling could be broadly defined as any instance that a cell takes on water over acute or chronic timescales, resulting in a volume increase with shift to a more rounded morphology. The time frame of cellular swelling onset and resolution is dependent on the duration of

the physiological or pathological stimulus together with engagement of volume regulatory homeostatic pathways which all cells possess (Jentsch, 2016). We would like to be careful not to blur the definition of cell swelling into something more akin to plasticity or cellular remodeling, which would have a slower onset, continue or persist long after the stimulus has subsided, and engage signaling pathways resulting in long-term changes in gene transcription, alteration of cytoskeletal proteins, and/or redistribution of ion channels and transporters. Just a few examples of astrocyte remodeling include retraction of glial processes in the supraoptic nucleus of the hypothalamus during the physiological response of parturition (Hatton et al., 1984; Theodosis et al., 2004), synaptic remodeling events during development (Bosworth & Allen, 2017; Chung et al., 2015), increased or decreased astrocytic ensheathment of synapses in response to LTP-like protocols (Genoud et al., 2006; Henneberger et al., 2020; Lushnikova et al., 2009; Tonnesen et al., 2018), and reprogramming of astrocytes into a reactive state in response to brain injury or disease (Hamby et al., 2012; Sofroniew, 2020; Watkins & Sontheimer, 2012). Of course there is a place where plasticity and cell swelling will intersect, for example long term changes in expression of astrocytic AQP4 channels, volume-regulating channels, K^+ channels, ion cotransporters or pump proteins which can result in more pronounced or weakened volume responses. As will be discussed in detail, glial cells have been implicated in cell swelling responses of nervous tissue across a physiological range of potassium concentrations or neuronal stimulation, while the bulk of evidence suggests that neurons contribute to swelling of brain tissue in more pathological situations including cortical spreading depression, energy failure and excitotoxicity (Inoue & Okada, 2007; Rungta et al., 2015; Steffensen et al., 2015; Zhou et al., 2010).

Astrocyte volume regulates tissue excitability in a very fundamental way. Astrocyte volume during a resting, wakeful state could be considered a baseline or homeostatic set point for levels of brain tissue excitability. On one end of the spectrum during sleep or loss of consciousness, astrocyte volume is at its lowest point, opening up the extracellular space (ECS) for convective flow and removal of metabolic waste into the vascular system (Jessen et al., 2015; Xie et al., 2013). The expanded ECS during sleep increases diffusion and dilutes concentrations of ions and neuroactive molecules and neurotransmitters, lowering the set point for effective neuronal stimulation and activity (Nicholson & Hrabetova, 2017). As astrocytes swell above baseline volume, the volume of the ECS decreases, limiting diffusion of ions, small molecules, and neurotransmitters. As the ECS shrinks, the effective concentration of the excitatory neurotransmitter glutamate is elevated, increasing ionotropic glutamate receptor activation, neuronal depolarization and synchrony of neuronal firing (Lauderdale et al., 2015). Simply raising extracellular potassium concentration by ~5 mM decreases the size of the ECS and triggers electrographic seizure activity in the CA1 region of hippocampus (Traynelis & Dingledine, 1988). Even in conditions in which synaptic activity is blocked pre- and post-synaptically (low $[Ca^{2+}]$, EGTA, DNQX, AP5), cell swelling can elicit epileptiform activity in slices (Dudek et al., 1990). This suggests a direct correlation between tissue swelling and brain tissue excitability. Using a technique called fluorescence recovery after photobleaching (FRAP), the diffusional capacity of the ECS was quantified in vivo using anesthetized mice with open craniotomy. During either administration of water i.p. or the pro-convulsant drug PTZ, ECS diffusion was hindered in the mouse cortex, sometimes promoting dead-space microdomains in the cortical tissue that occurred *prior* to seizure initiation (Binder et al., 2004). In slices, application of hyperosmolar ACSF, which initiates expansion of the ECS by sucking water out of cells, has been shown to reduce or completely block epileptiform activity brought on by hypoosmolar ACSF (Kilb et al., 2006) or elevated extracellular K^+ (Traynelis & Dingledine, 1989). In other models of epilepsy, such as low-$[Mg^{2+}]$ ACSF application to hippocampal slices, decreases in osmolarity lead to increased seizure duration, while increases in osmolarity produce the opposite effect (Shahar et al., 2009). The hypoosmolar model of cell swelling generates excitatory currents in CA1 hippocampal neurons, even in the presence of tetrodotoxin to block synaptic activity. These events, known as slow inward currents (SICs), are NMDA receptor dependent, as they are nearly abolished in the presence of the NR2B subunit selective NMDA receptor antagonist Ro 25-6981 (Lauderdale et al., 2015). Further single-cell imaging experiments in slices have shown that astrocyte swelling directly precedes the onset of SICs in the hypoosmolar model of acute cellular edema (Murphy, Davila, et al., 2017). Thus, astrocyte swelling above the baseline state is directly tied to neuronal excitability increases, and in the extreme can push tissue excitability into a pathological state triggering seizures. Suggested mechanisms underlying astrocyte swelling-mediated neuronal excitability increases have been reviewed previously (Murphy, Binder, and Fiacco 2017).

Astrocyte swelling can also contribute to brain pathology, and has been observed in a number of disease models where long-term changes in astrocyte channels and/or transporters leave them in a chronically swollen state and/or more prone to swelling. The excessive energy demands of the brain require adequate flow of oxygen and glucose, which are transported to cells via arterioles and capillaries. Minimal intercapillary distance (MID) is important for ensuring rich oxygenation and nutrient supply to tissues. With astrocyte swelling, distortion of the tissue landscape dramatically reduces neuronal access to the vasculature by increasing MID, putting a strain on the resources of nearby neurons and increasing the risk of hypoxia and necrosis (Bourke et al., 1980). In a mouse model of acute liver failure, the development of hyperammonemia leads to cerebral edema, largely mediated by the swelling of astrocytes (Lichter-Konecki et al., 2008). Cerebral edema is characterized by increasing intracranial pressure (ICP) and elevated brain water content, which enters the tissue through the aquaporin-4 enriched astrocytic endfeet apposing the vasculature. Upregulation of AQP4 is known to increase the severity of vasogenic edema by facilitating the movement of water into the brain parenchyma via the astrocyte endfeet (Yang et al., 2008). After injury and during neurodegeneration, astrocytes are known to develop reactive phenotypes, which can undergo maladaptive dysregulation of key channels normally expressed at the endfeet, precipitating swelling (Wetherington et al., 2008). After ischemia in the retina, swollen

astrocytes have been shown to down-regulate potassium conductance and redistribute Kir4.1 channels away from the vasculature (Pannicke et al., 2004). This swelling can be appreciated clinically with diffusion-weighted imaging and is a hallmark in scans after traumatic brain injury (Badaut et al., 2011). In the rare megalencephalic leukoencephalopathy with subcortical cysts (MLC) disease, the defective MLC1 protein alters the ability of astrocytes to regulate their volume, with further progression leading to white matter swelling abnormalities (Bugiani et al., 2017). After transient ischemia, the widely-expressed volume regulated anion channel (VRAC) is activated in astrocytes during swelling and releases glutamate, contributing to an excitotoxic environment (Yang et al., 2019; Zhang et al., 2008). When delivered by intracisternal microdialysis, the VRAC inhibitor 4-[(2-Butyl-6,7-dichloro-2-cyclopentyl-2,3-dihydro-1-oxo-1*H*-inden-5-yl)oxy]butanoic acid (DCPIB) reduced glutamate in the CSF as well as infarct size in a model of stroke (Zhang et al., 2008). Similarly, in a transgenic mouse model, conditional ablation of VRAC also effectively reduced infarct size following stroke (Yang et al., 2019). These studies illustrate the impacts of cell and brain tissue swelling in modulating neuronal excitability and overall health and survival of brain tissue in injury and disease.

2 | MEASUREMENTS OF CELL SWELLING

Various techniques have been used to measure cell volume directly or indirectly (summarized in Figure 1). In the vast majority of studies, the actual volume of cells is not measured. Cell volume alterations have been inferred indirectly by measuring intrinsic optical signals (IOS), changes in extracellular ion concentrations, or volume/resistance of the ECS. With ongoing improvement in microscopy and imaging tools and software-based analysis programs, the field has moved increasingly towards visualization of the astrocytes or neurons themselves to quantitatively assess their volume—although even these methodologies have their limitations. What implications this may have for the field are likely also rooted in how data are analyzed, so that quantitative predictions contain minimal variability and are therefore more reproducible between groups.

2.1 | Extracellular tissue resistance

One indicator of cell volume change is tissue resistance, recorded by microelectrodes placed within the ECS of intact brain tissue (Traynelis & Dingledine, 1989). According to Ohm's Law:

$$V = IR,$$

where V refers to voltage, I refers to current, and R refers to resistance.

Thus, to record changes in ECS resistance, a stimulating electrode generates electric current, while recording electrodes in the ECS measure ΔV between electrodes. With this information, tissue resistance can be calculated as:

$$\Delta R = \frac{\Delta V}{I}.$$

Over time, this imparts information regarding the shrinkage or expansion of the ECS during an experiment. This technique was used by Traynelis and Dingledine to record the effects of elevated extracellular K^+ on seizure activity in rat hippocampal slices (Traynelis & Dingledine, 1988, 1989). These studies revealed the critical role of cell swelling (presumed to be astrocytic) in recurring ictal or seizure-like activity.

2.2 | Membrane permeant & impermeant probes

Membrane impermeant probes are a useful tool that have been used to make measurements relative to space or concentration of units within a space. Modern studies continue to supplement experiments with these techniques, as they are a dependable method for making predictions about volume change occurring in bulk tissue. One such probe is the radioactive 3-O-methyl-D-glucose (3OMDG), which is a permeable molecule that crosses the membrane via the facilitated diffusion mechanism normally utilized by sugars. Because 3OMDG transport is entirely concentration-dependent, flux will stop at equilibrium between the ECS and intracellular compartments. Therefore, bulk changes in radioactive content between compartments are the result of volume change in response to a treatment. This technique was used in cultured astrocytes to measure intracellular volume (Kletzien et al., 1975). However, flux of 3OMDG could be a confounding variable when measuring osmotic gradients during experiments, which lessens the appeal of this measurement approach. Application of phloretin can trap 3OMDG inside cells, a property that could be useful for retaining the volume of a cell at a given point in time (Kletzien et al., 1975).

Another method relies on monitoring the concentration of the cation tetramethylammonium (TMA^+). Potassium-sensitive microelectrodes normally record changes of $[K^+]_o$ in intact tissue, but encounter strong electrical interference when exposed to TMA^+ solutions. The magnitude of this interference can be used to calculate relative $[TMA^+]$ in the ECS (Dietzel et al., 1980; Nicholson et al., 1979). The volume of the ECS is negatively correlated with $[TMA^+]$, as shrinkage of the ECS increases $[TMA^+]$. Importantly, TMA^+ cations are impermeable to cellular membranes on short timescales, allowing changes in $[TMA^+]$ to faithfully represent changes in ECS volume. Choline (a similar agent) and TMA-sensitive electrodes have widely been used historically (Hrabetova et al., 2003; Medina et al., 2007; Ransom et al., 1985; Sykova & Nicholson, 2008) and remain in use in today (Bai et al., 2018; Larsen et al., 2014; Larsen & MacAulay, 2017) to measure ECS volume changes. Tortuosity values can also be calculated using both $[TMA^+]$ and diffusional capabilities in the ECS. Changes in tortuosity relate to changes in both the landscape and volume of the ECS, where diffusion of TMA^+ cations may be impeded by physical structures in the neuropil (Kilb et al., 2006). One unfortunate aspect of this technique requires insertion of the electrodes into

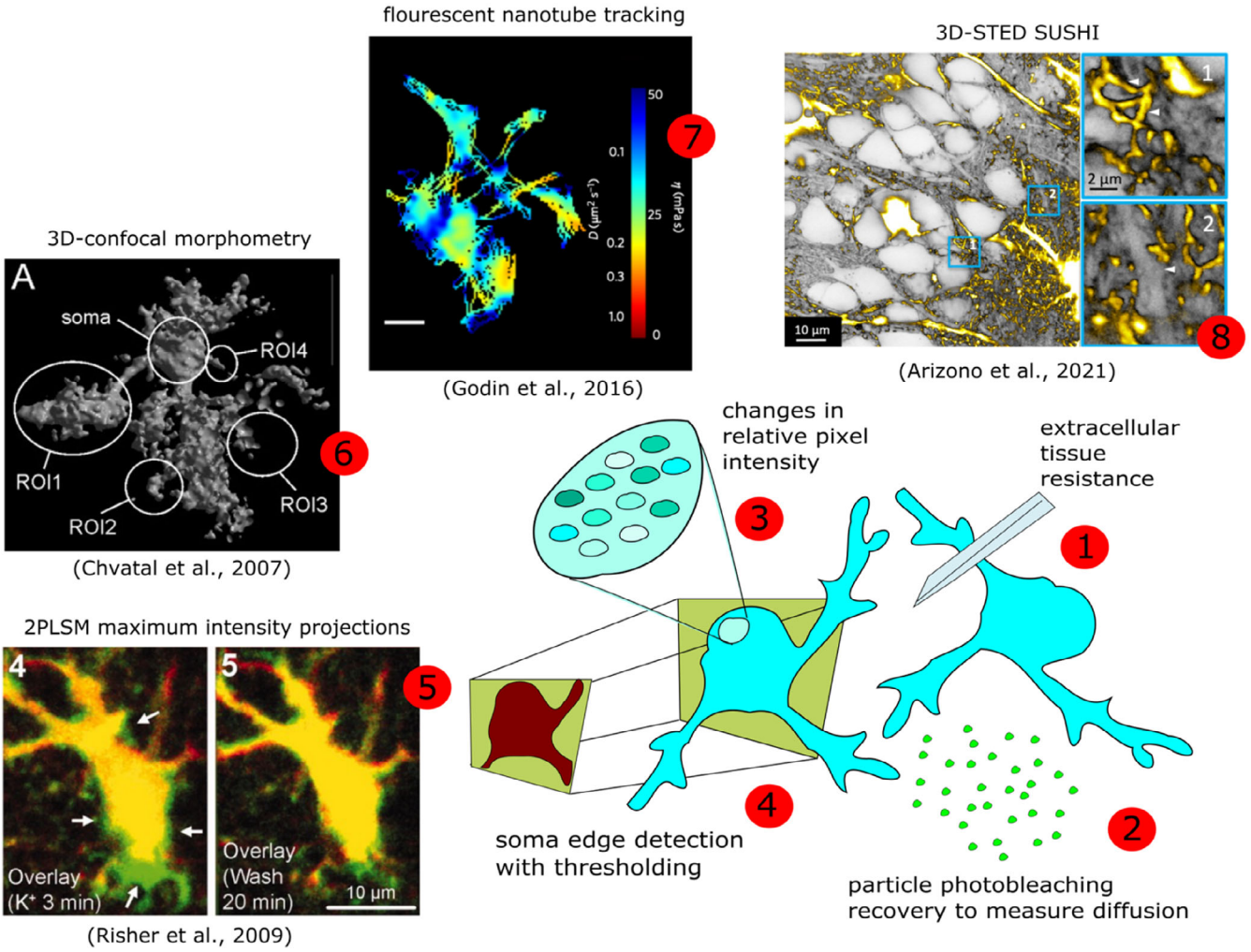

FIGURE 1 Summary of techniques to measure or estimate astrocyte swelling. (1) Increases in extracellular tissue resistance indicate reduction in the volume of the ECS, which is inversely correlated to cell volume changes. (2) Recovery of fluorescent indicator in the ECS after photobleaching. Slowed diffusion rates are indicative of constricted ECS. (3) Dimming of cytosolic fluorescent indicator is an indicator of cell swelling due to dilution by water, while increased signal intensity results from cell shrinking. (4) Real-time volume measurements in fluorescently labeled cells through edge detection of binarized images overlaid over the baseline image (see Figure 2). (5) Example of real-time volume measurement in an astrocyte. An image taken after 3 min in 26 mM K^+ is overlaid onto the baseline image, with expansion of the cell border marked by the arrows (4), followed by recovery to baseline volume after washout of high K^+ (5) (from Risher et al., 2009). (6) 3D confocal morphometry is similar to real-time volume imaging in its use of *z*-stacks and edge detection with thresholding, but with some notable differences. Rather than thresholding after *z*-stack compression, in 3D morphometry unit areas are calculated for each thresholded image individually and converted to square microns, summed, and multiplied by the distance between neighboring sections in the stack. A number of additional image processing steps are also applied, including correction for photobleaching due to the larger *z*-stacks (50–60 individual sections) and duration of recordings (up to 80 min). For details, see Chvatal et al., 2007. 3D morphometry offers improved spatial resolution at the expense of temporal resolution, enabling imaging in bulk astrocyte processes. (7) Luminescent single-walled carbon nanotubes can be tracked over long timescales to measure variances in the local architecture of the ECS (from Godin et al., 2017). Presumably, movement of the nanotubes would be hindered by cell swelling-induced compression of the ECS. (8) Super-resolution shadow imaging (SUSHI) combined with fluorescent labeling of astrocytes enables simultaneous measurement of local pools of ECS and individual astrocytic perisynaptic processes. SUSHI offers data collection at rapid timescales and with unprecedented spatial resolution (from Arizono et al., 2021).

tissue, thereby introducing damage into the site of observation prior to the start of experiments. Additionally, this measure does not give any information about swelling of different cell types that may be contributing to changes in ECS volume.

Another method enables the measurement of diffusion of high molecular-weight fluorescent dextrans in the ECS, which provides information about molecular constriction and crowding around astrocytes. The introduction of the fluorescein isothiocyanate (FITC)-labeled dextrans can be performed in a minimally invasive and in vivo procedure (Binder et al., 2004). The ACSF-dissolved molecule is loaded onto the exposed dural surface of a mouse, post-craniectomy. Photobleaching of the FITC molecules is performed, and FRAP data is acquired over time points after the bleaching pulse. Slower FRAP values indicate reduced diffusion in the ECS, and subsequently can

identify dead space microdomains. This is an important tool, as it can reveal differences in subcompartments of the ECS as opposed to ECS volume as a whole. Another advantage of this technique includes the various molecular weights of dextrans that can be used to quantify information about how ECS diffusion is affected by swelling.

Membrane-permeant fluorescent probes have also been used to visualize and record changes in astrocyte volume based on changes in fluorescence intensity. Hansson et al. (1994) used a Pluronic acid buffer to solubilize the fluorophore fura-2/AM for passive uptake into cells; similarly, calcein-AM can be used (Gunnarson et al., 2008; Zelenina & Brismar, 2000). Enzymatic cleavage of the AM ester yields it membrane impermeant once inside the cell. The cells loaded with indicator can then be measured for fluorescence intensity. Any changes in this value are proportional to changes in intracellular water content, such that fluorescence intensity decreases with increasing intracellular water content and vice-versa. This "dimming" of fluorescence intensity was used by Murphy, Davila, et al. (2017) as an alternate method to measure volume changes of neurons located deep in tissue that was otherwise difficult to quantify using thresholding analysis.

2.3 | Light microscopy and intrinsic optical signals (IOS)

Basic light microscopy can be used on isolated cells in culture to estimate cell volume changes based on changes in cross-sectional area. In a study using differential interference contrast (DIC) optics, cross-sectional images were analyzed on the basis of soma area, and distance of (visible) processes from the soma (Su, Kintner, & Sunl, 2002). [Corrections added on June 16, 2022: Ritchie, Glusman, & Haber, 1981, has been changed to Su, Kintner, & Sunl, 2002.] Changes in these areas or distances over the course of treatment were considered estimates of volume change. Encouragingly, a decrease in osmolarity of solutions applied to astrocyte cultures was correlated with an increase in the cross-sectional areas of astrocytes. This technique was used to evaluate mechanisms of cultured astrocyte swelling responses to 75 mM potassium.

While still controversial, many laboratories have relied on intrinsic optical signals as a reporter for morphological tissue changes in the brain. As cellular volume increases in the tissue, the amount of light scattering decreases, resulting in a change in IOS that corresponds to change in bulk cell volume. The measurements are taken at relatively low magnification and therefore provide an indication of bulk swelling (or shrinking) of tissue at low resolution. The challenge in using IOS data involves making assumptions as to the physiological triggers of the optical phenomenon. Some groups attribute IOS to very specific changes in the tissue, while others argue that the signals can be generated from multiple biological processes. In one of the early studies by Andrew and MacVicar (1994), it was shown that stronger IOS (increased light transmittance) could be observed during an experiment with hypotonic and high-potassium application to astrocytes. This provided early evidence that changes in IOS corresponded to increased light transmittance, and presumably cell swelling. Other groups have used this technique to measure astrocyte volume changes with apparent success (e.g., Holthoff & Witte, 1996), and the utility of an endogenous swelling reporter system saved time and resources.

To critically evaluate the technique, another group compared IOS signals to [TMA^+] measurements in the ECS, as well as other relevant factors (Sykova et al., 2003). The authors found that in response to neuronal stimulation, TMA and IOS measurements of astrocyte swelling did not correspond temporally. The IOS signals did not appear to correlate with increasing potassium concentration, even though increasing potassium has been shown to induce swelling. Furthermore, IOS signals did not match other parameters used to assess swelling or ECS shrinkage, such as tortuosity or diffusion coefficients. A more recent study took a broader definition of IOS, and simply correlated changes in tissue light scattering as an output for cell morphological change (Kitaura et al., 2009). In summary, the challenge in using this form of measurement lies with the broad interpretation of IOS, its low resolution, lack of cell-specific volume estimates, and the lack of corroboration with other cell volume measurements.

2.4 | Florescence microscopy real-time volume imaging and analysis

The progression of fluorescence microscopy techniques and development of transgenic fluorescent tools has enabled groups to characterize astrocyte morphology with sufficient resolution to make definitive conclusions about cell volume changes in response to stimuli in real time. Methods to fluorescently label cells are many, including use of permeant indicators such as AM dyes, Sulfarhodamine-101 (SR-101), dialysis of single cells via patch clamp with cytosolic dyes of varying wavelengths, to transgenic expression of fluorescent reporters using cell-type specific promoters. Current optical and analysis limitations dictate that conservative estimates be integrated into the analysis to prevent predictions of volume change of structures beyond the image resolution. Despite these challenges, current analysis methods are rapidly improving. A common theme to many imaging protocols relies on taking stacks of images in the *z*-axis through the entire cell and recompiling them to perform analysis of volume change during treatments (Figure 2).

In one such study, a series of images was collected along the *z*-axis in rapid succession through astrocytes expressing eGFP under the control of the human glial fibrillary acidic protein (GFAP) promoter (Chvatal et al., 2007). This process was repeated over a desired time course, and the subsequently generated *z*-stacks were flattened and filtered by imaging software. The soma and large processes were then analyzed by a method called thresholding, wherein pixels above and below certain intensities are assigned grayscale values, thereby binning the pixels into manageable groups. After thresholding, the areas of the soma and processes were calculated using a method called edge detection, which involves software recognition of sharp changes in brightness within the image. At these points of contrast, lines are generated to form an edge, which presumably will define the area of

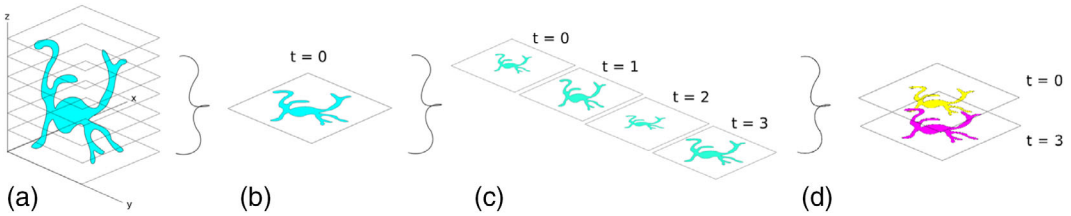

FIGURE 2 Real-time volume measurements. Morphometric analysis of fluorescently labeled cells begins with the collection of a *z*-stack of images at one point in time (a). Image processing allows for compression of the *z*-stack into a single optical section (b), where all of the *z*-axis pixels are flattened onto a single plane. Compressed *z*-stacks are collected across individual timepoints (c), and methods such as edge detection after thresholding of average or maximum intensity projections are used to estimate cellular volume changes in the overlaid images (d). The temporal resolution is limited by the time needed to acquire each individual *z*-stack, but 1 min intervals are achievable at sufficient signal-to-noise to permit accurate edge detection of the soma and major processes despite dimming of cytosolic indicator (Lauderdale et al., 2015; Murphy, Davila, et al., 2017).

the astrocyte. Similar procedures have been used by many labs using both confocal (Benesova et al., 2012; Murphy, Davila, et al., 2017) and higher resolution two-photon laser scanning microscopy (Dibaj et al., 2007; Florence et al., 2012; Nase et al., 2008; Risher et al., 2009), with slight variations. With rapid scanning features, optical stacks through astrocytes can be generated in 15–20 s or less, enabling minute-by-minute assessment of rapid cell volume changes (Walch et al., 2020). Availability of transgenic mice with fluorescent reporters expressed downstream of a cell-type specific promoter such as Thy-1-eGFP for pyramidal neurons or lox-stop-lox (lsl)-TdTomato for specific Cre lines may offer improved signal-to-noise over bulk dyes or other cytoplasmic indicators.

Some protocols have used maximum intensity projections (Florence et al., 2012; Murphy, Davila, et al., 2017; Risher et al., 2009) for the compilation of *z*-stacks, which allows for greater image dimensionality. This is a technique that is commonly used in radiology specialties such as positron emission tomography. In some cases, a fixed space is defined in which apparent volume changes will be measured, while others manually draw regions of interest (ROIs) during the analysis process. This is a step in which group-to-group variability may become amplified, and as such can present a problem for reproducibility of data. For example, Nase et al. (2008) chose to perform deconvolution on collected *z*-stacks and reassemble them into 3D formulations, where volume of the astrocyte could then be calculated in real-time. In the work of Kirov and colleagues (Andrew et al., 2007; Risher et al., 2009), four separate methods were used to measure cell volume: 1) Comparison of gray value pixel distributions, where an increase in the proportion of white pixels (representing GFP staining) signified an expansion of the imaged structure into adjacent space, assuming overall brightness remained constant; 2) Control profiles of somata in stacked images digitally traced by hand and filled to create a mask from behind, through which swelling could be discerned; 3) Overlay of pseudocolored control and experimental image stacks; and 4) Measurement of changes in a polygonal area drawn by linking cellular landmarks, where an expanding polygonal area indicated components moving apart in space (Andrew et al., 2007). Between the two studies, there was a chronological shift away from analysis of gray value pixel distributions in favor of overlay of pseudocolored maximum intensity projections (MIP), illustrating refinement in analysis strategy. This shift in strategy is noteworthy in that, using the newer technique of overlay of thresholded MIP image stacks, 2017; Murphy, Davila, et al. (2017) found clear evidence of rapid neuronal swelling in hypoosmolar conditions where Andrew et al. (2007) reported no neuronal volume change based on analysis of gray value pixel distributions.

Both the Kirov and Nase groups commented on the limitations of existing microscopy technologies, given that most astrocyte processes are beyond the resolution of even two-photon microscopes. Another shared grievance involved the effects of tissue swelling on image distortion, wherein the astrocyte itself becomes harder to track and easily lost (Nase et al., 2008). As the field awaits improved image resolution, labeling and detection tools, an achievable goal may be to standardize the image analysis process, so that data can be more easily compared within and across labs with minimal bias.

2.5 | Limitations of real-time volume imaging & new directions to measure astrocyte volume changes: Super-resolution microscopy and super-resolution shadow imaging

Studies using real-time volume imaging of fluorescent astrocytes to directly measure cell volume changes have been limited mainly to analysis of the soma. Some imaging of large astrocyte processes or a large field of smaller processes has been possible using strong swelling paradigms over longer timescales (10–20 min), but with increased variability of responses between selected regions of interest (Benesova et al., 2012; Chvatal et al., 2007; Dibaj et al., 2007). Dibaj et al. (2007) chose to measure visible processes within a fixed distance of the astrocyte soma. Their results after 10 min in 33% hypoosmolar ACSF suggested that Kir4.1 may play a role in volume regulation in the processes, but not in the soma. Anderova, Sykova, and colleagues were able to categorize different classes of astrocytes based on swelling phenotypes involving the processes and soma after either prolonged oxygen–glucose deprivation (OGD) or exposure to 33% hypoosmolar ACSF (Benesova et al., 2012; Chvatal et al., 2007). In "low-response astrocytes," swelling in the processes was the same as in the soma, whereas in "high-response astrocytes" the swelling of the processes

was greater than in the soma. Although these studies have been limited to large processes or bulk imaging of a field of smaller processes, these studies suggest that the soma and processes may have differing swelling responses and volume regulating mechanisms. Beyond current reach of confocal or standard 2-photon imaging approaches is visualization of ultrafine structures in astrocytes, such as the fine branching processes in close proximity to synapses which have been estimated to be 30–50 nM across (Lehre & Rusakov, 2002; Ventura & Harris, 1999; Witcher et al., 2007). The emergence of super-resolution microscopy has started to bridge this gap. Nagerl and colleagues recently developed a modified stimulated-emission depletion (STED) microscopy approach called super-resolution shadow imaging (SUSHI) to estimate volume changes in local ECS compartments (Tonnesen et al., 2018). Rather than labeling cells with a fluorescent indicator, this technique involves filling the ECS with indicator instead and inverting the image to create a high contrast relief of the ECS against the backdrop of cells and neuropil which appears white. Aside from the advantage of reducing photobleaching as compared to cellular labeling, this technique allows for unprecedented spatial resolution of sheets and tunnels of ECS around cellular compartments including dendrites, spines, and perisynaptic astrocyte processes. By combining SUSHI imaging with fluorescent labeling of individual astrocytes, Arizono et al. (2021) measured changes in localized regions of the ECS within small ring-like structures of astrocyte processes, presumably encapsulating local pools of ECS or dendritic spines. Upon experimental osmotic challenge, astrocytic microstructures remodeled and swelled up at the expense of the pools, effectively increasing the physical interface between astrocytic and cellular structures. Direct measurement of astrocyte processes (called shafts) making up a portion of the ring-like structures revealed consistent expansion upon hypoosmotic challenge, increasing in diameter from 204–231 nm in response to a 30% reduction in solution osmolarity. This work has provided an exciting step forward by enabling simultaneous measurement of changes in the ECS and astrocyte processes that are corroborative; i.e. the swelling of local astrocyte processes is verifiable by simultaneous reduction of the ECS or compression of microstructures. Future utilization of this technique can be used to assess and compare swelling responses in fine structures to the soma to determine if changes are uniform in nature or are locally regulated depending upon the complement of transporters, pumps, or ion channels expressed in different parts of the cell.

3 | MECHANISMS OF ASTROCYTE SWELLING

3.1 | Common experimental models to induce cell swelling

In efforts to identify mechanisms underlying astrocyte swelling, there are notable discrepancies between results that likely stem from different swelling models and methodologies of measurement. Astrocyte swelling has been induced using in a variety of experimental conditions spanning the physiological to pathological. This range of conditions has run from: 1) mild to moderate levels of synaptic activity modeled by stimulation of neuronal afferents such as the Schaffer collaterals in the hippocampus; 2) sustained bath increases in extracellular K^+ concentration within a physiological range from a few millimolar up to 10–15 mM, which approaches ceiling $[K^+]_o$ levels observed during seizure; 3) models of brain injury such as stroke by OGD; or 4) use of very high concentrations of extracellular $[K^+]_o$ which may occur either transiently during spreading depression, or more sustained in cases of energy failure or excitotoxicity. In the more pathological situations it is clear that neurons also participate in rapid swelling responses (Andrew et al., 2007; Rungta et al., 2015; Zhou et al., 2010).

The most commonly used model of cell swelling is application of hypoosmolar ACSF made by either simple dilution with distilled water or removal of NaCl from the extracellular medium. Hypoosmolar solutions have been described as ranging from mild to severe in terms of percent reduction (17% to up to 60%). This model is particularly intriguing in that it introduces an instantaneous osmotic gradient across the cell membrane, as opposed to water movement coupled to permeation or transport of ions or small molecules. Severe hypoosmolarity provides a useful model for pathological situations such as hyponatremia or water intoxication. For the scope of this review, we will focus attention on mechanisms of astrocyte swelling associated with elevated extracellular K^+, as would be expected to occur during varying levels of neuronal activity. Most of the transmembrane pathways theorized to contribute to astrocyte swelling in elevated $[K^+]_o$ are reviewed individually, but can be visually summarized in Figure 3. The hypoosmolar model will be revisited briefly, specifically in the context of water movement.

3.2 | Early theories on potassium buffering and effects on the brain extracellular space

Current knowledge of astrocyte swelling is built upon early studies characterizing ion composition of the ECS. Even in early studies, it was observed that neuronal excitation brought about increased K^+ permeability in neighboring glial cells (Lundandersen & Hertz, 1970). A coupling of sodium and potassium in the medium was observed to be necessary for an intracellular accumulation of potassium to trigger swelling (Lundandersen & Hertz, 1970). Similarly, it was observed that electrical stimulation of nerve cells could trigger glial swelling. In further experiments with sustained stimulation of neurons nearing epileptic bursting frequency, a continuous increase of potassium was measured in the extracellular space (Dietzel et al., 1980). This concentration of potassium was far above the "ceiling level" thought to border between 10–15 mM. The way in which glia were thought to respond to such high concentrations of potassium was termed spatial buffering, a process in which $[K^+]$ itself does not change, but potassium ions are redistributed from sources to sinks (Ballanyi et al., 1987). There would be a conservation of ions and a displacement of their location from sites of high neuronal activity to glia

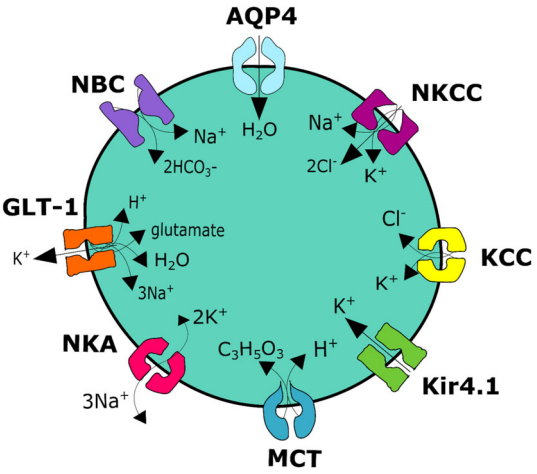

FIGURE 3 Transmembrane proteins involved in astrocyte swelling in elevated $[K^+]_o$, along with their substrates. All have the potential to move substrates outward as well under certain conditions. Aquaporin-4 has been tested in many in vivo models in comparison to the other proteins shown. Potassium inwardly rectifying channels are supported by the classical potassium siphoning hypothesis, while the sodium-potassium ATPase has received renewed attention in recent studies due to the uniquely K^+-sensitive isoform expressed by astrocytes. The sodium-potassium-chloride and potassium-chloride cotransporters are strongly supported by primary culture experiments performed using pathological potassium concentrations, but may be less physiologically relevant than the other proteins. Other evidence points to a role for the sodium bicarbonate cotransporter NBCe1 and monocarboxylate cotransporters (MCT1 and 4) at $[K^+]_o$ levels closer to basal $[K^+]_o$. Evidence supports the astrocyte sodium-potassium pump as the main K^+ entry pathway in more elevated and sustained extracellular K^+ conditions. Key: Aquaporin-4: (AQP4); sodium potassium chloride cotransporter: (NKCC1); inwardly rectifying potassium channel: (Kir); monocarboxylate transporters: (MCT); sodium-potassium ATPase: (NKA); sodium bicarbonate cotransporter: (NBCe1)

in quiescent areas of the ECS. It was proposed that swelling might occur mainly via spatial buffering and the activity of the Na^+-K^+-ATPase (NKA) (Walz et al., 1984). Focus was placed on the theory that large water shifts might occur during the coupled transit of sodium and potassium across the membrane in a mechanism yet to be elucidated (Walz & Hinks, 1985).

Detailed characterization of the biophysical properties of Müller cells in the retina provided seminal knowledge that later carried important implications for K^+ conductance of glial cells in the CNS and provided evidence for the concept of spatial buffering. It was discovered that the endfeet of Müller glia possessed a higher resting K^+ conductance than other regions of the cell (Newman, 1986). This is perhaps one of the earliest indications that glia could differentially express ion channels in a region-specific manner. Newman further argued that by using internal pathways of high to low conductance regions in the Müller cell, potassium ions are not so much spatially buffered, as much as siphoned. Spatial buffering lacked a directional relationship, while $[K^+]$ siphoning alluded to the push-pull relationship directing ionic currents and fit with the nearly instantaneous increase in K^+ conductance at the endfeet upon application of K^+ to the other end of the cell. Newman suggested that K^+ siphoning by Müller glia in the retina directed potassium into the vitreous humor in a mechanism that might parallel how brain astrocytes direct excess potassium into capillaries at their endfeet. This suggested that buffering is not simply a homogenous diffusive capacity of astrocytes, but an ability to direct potassium from individual sources to a shared 'sink', such as a nearby capillary.

It was proposed that potassium inwardly-rectifying (Kir) channels might be best suited to initiate siphoning of potassium into glia during physiological conditions based on their preferred conductance during hyperpolarization (Kofuji et al., 2000). Orkand supplemented Newman's hypothesis, proposing that the Nernst potential for potassium would affect the flux through Kir channels such that the initial influx of potassium would depolarize the surrounding membrane enough to reduce—but not reverse—the inward driving force on potassium in the locally high $[K^+]_o$ region. As potassium would conduct through the astrocyte towards the endfoot region, the now depolarized membrane would direct the driving force for potassium outward through Kir and into the apposed vasculature (Ballanyi et al., 1987). After potassium movement into the vasculature, the maintenance of the membrane potential via NKA would be important to return to homeostatic conditions. This early work and the role of Kir channels in spatial buffering and siphoning of K^+ became the prevailing theory behind extracellular K^+ regulation.

3.3 | Kir4.1 and AQP4: A mechanism for K^+ and water entry or exit from astrocytes?

Work on potassium buffering and associated water movement was reinvigorated by a study detailing an impressive localization of the water channel aquaporin-4 (AQP4) to the endfeet bordering the vasculature in comparison to sparse expression facing the neuropil (Nielsen et al., 1997). The selective and polarized expression of AQP4 in astrocytes supported the complimentary theories of Newman and Orkand, as the Kir channels could provide the solute movement necessary to pull water into astrocytes via AQP4 channels to support K^+ spatial buffering and give astrocytes a unique role in water handling in the brain in both physiological and pathological conditions.

Subsequent work on Kir4.1 channels and AQP4 provided additional perspective on their potential roles in K^+ siphoning and effects on ECS volume. Kofuji et al., (2000) found differences in regional distribution of Kir4.1 and Kir2.1 in Müller glial cells of the mouse retina suggesting that weakly-rectifying Kir4.1 might be best suited to allow K^+ to exit to large sinks such as the vitreous humor and surrounding retinal blood vessels. The role of Kir4.1 in K^+ buffering was questioned by the work of Meeks and Mennerick (2007), who found that even though $BaCl_2$ at 100 μM blocked the stimulus-evoked K^+ current in astrocytes, it did not affect local concentrations of extracellular K^+. More recently, Larsen et al. (2014) reported that Ba^{2+} block of astrocytic Kir4.1 did not significantly alter extracellular K^+ kinetics or contribute to extracellular space volume reduction resulting from high frequency stimulation in the hippocampus. However, locally-

applied K^+ by iontophoresis in the presence of Ba^{2+} consistently generated an increase in peak K^+ without affecting post-stimulus decay of $[K^+]_o$. In stronger swelling models, the role of Kir4.1as an exit route for K^+ into large sinks became more apparent. Using time-lapse two-photon microscopy in spinal cord slices, Dibaj et al. (2007) observed prominent swelling of larger astrocyte processes during co-application of hypotonic solution and Ba^{2+} to block Kir, but not in hypotonic solution alone. These observations were replicated in Kir4.1$^{-/-}$ mice, suggesting a role for Kir4.1 in *prevention* of glial process swelling during osmotic stress (Kofuji et al., 2000). Similar observations have been made in the retina. Wurm et al. (2006) found that swelling of Müller glia is dependent upon maturation of Kir4.1 channels. Immature glia that have not yet developmentally upregulated Kir4.1 expression exhibited prominent swelling, whereas mature Müller glia did not. Furthermore, upon pharmacologic block with Ba^{2+}, mature Müller cells swelled similarly to immature cells. The fact that immature glia that do not express Kir4.1 prominently swell is a strong indication that Kir4.1 is important for efflux of K^+ (and water) from the cell rather than uptake of K^+ in these conditions. The authors concluded that functioning Kir channels are required for rapid osmotic volume *regulation* (Wurm et al., 2006), similar to what has been described for volume-regulated anion channels (Jentsch, 2016).

Similar observations have been made with regard to the role of AQP4 in water movement. A follow-up study to that of Nielsen et al. (1997) by the Ottersen group conducted in a glial fibrillary acidic protein (GFAP)-driven conditional knockout of AQP4 (cAQP4$^{-/-}$) showed that indeed, astrocytes express AQP4 and not the endothelial cells of the vasculature (Haj-Yasein et al., 2011). Water loading experiments in these mice showed cAQP4$^{-/-}$ astrocytes had decreased uptake of water, but the total brain water content was burdened in comparison to AQP4$^{+/+}$ mice. These findings suggested that AQP4 is important for both influx and efflux of water, and that astrocytes might act as a privileged gating mechanism to control the volumes of the ECS and vasculature. Another AQP4$^{-/-}$ brain slice experiment tested weak versus strong stimulation of neurons to vary the potassium concentration physiologically (Strohschein et al., 2011). The AQP4$^{-/-}$ slices had reduced K^+ uptake near basal $[K^+]_o$ in comparison to wild-type slices, but stronger stimulation elicited similar levels of potassium uptake in AQP4$^{-/-}$ and wild-type slices. These experiments suggested that Kir4.1 and AQP4 may be more involved in K^+ and water entry around resting $[K^+]_o$ rather than at higher concentrations. Haj-Yasein et al. (2012) found that AQP4$^{-/-}$ astrocytes actually had more activity-induced ECS shrinkage in comparison to wild-type, suggesting increased cell swelling in AQP4$^{-/-}$ astrocytes. The authors suggested that this would occur if activity-coupled cotransport of water into perisynaptic glia normally is associated with a passive, AQP4-mediated water flux in the opposite direction. Recently it was published that selective inhibition of AQP4 with the drug TGN-020 failed to inhibit stimulus-induced extracellular space shrinkage in hippocampal slices (Toft-Bertelsen et al., 2021). In our own work, we have found that AQP4 is not required for astrocyte volume increases in either hypoosmolar (Murphy, Davila, et al., 2017) or raised extracellular K^+ conditions (Walch et al., 2020). Furthermore, AQP4$^{-/-}$ astrocytes actually swelled more than wild type, suggesting a role for AQP4 in exit of water from astrocytes in more extreme swelling conditions. Collectively, the above studies largely support the K^+ siphoning model of Newman in brain astrocytes. During very local and transient increases in $[K^+]_o$ (illustrated in Figures 4a and 5a), Kir4.1 and AQP4 might participate in K^+ and water clearance from the ECS that does not result in definitive changes in the ECS or cell swelling. During more sustained increases in $[K^+]_o$ (illustrated in Figures 4B and 5B-D) resulting in measurable cell swelling or ECS constriction, the findings support a role for Kir4.1 and AQP4 in siphoning of K^+ and

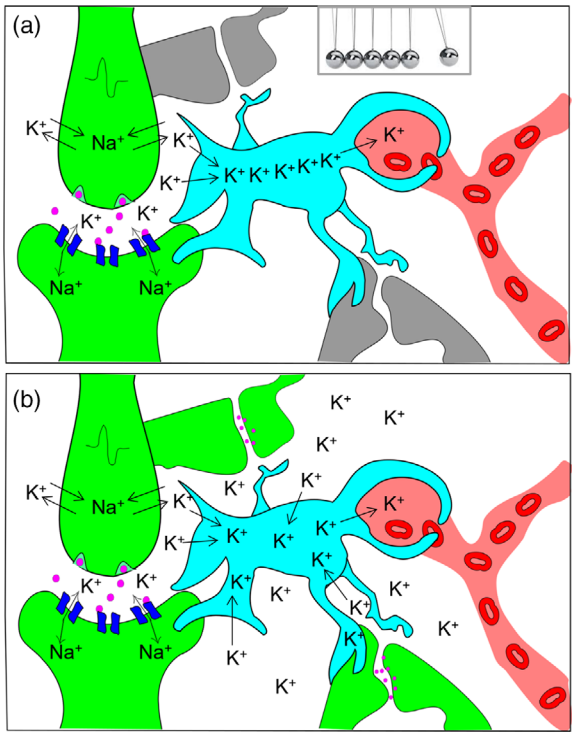

FIGURE 4 Local/transient versus sustained models of astrocyte swelling. (a) In many studies, low-level stimulation of neuronal afferents is used to generate local increases in $[K^+]_o$. Potassium is released presynaptically from voltage-gated potassium channels and postsynaptically from neurotransmitter-gated ion channels (receptors in dark blue, neurotransmitter pink) resulting in transient and local increases in $[K^+]_o$. Extruded potassium ions will enter the perisynaptic astrocyte processes and either released back into the ECS at areas of lower $[K^+]_o$ or siphoned into the vasculature at astrocyte endfeet. This local uptake and redistribution of potassium fits more closely with classical K^+-buffering/siphoning models. A Newton's cradle analogy could be used to model this type of K^+ movement (inset). Because the siphoning of K^+ out of the cell occurs almost concurrently with K^+ influx (Newman et al., 1984), it is not clear whether such an instantaneous electromotive (rather than diffusional) redistribution of K^+ would result in any appreciable or detectable swelling. (b) High frequency stimulation or models using bath application of potassium will produce more sustained, non-directional K^+ increases that will engulf the cell. In these instances, other K^+ handling mechanisms are activated resulting in increased intracellular K^+ concentration and readily detectable cell swelling using standard confocal and 2PLSM fluorescent imaging techniques. Active synapses are depicted in green. Specific swelling mechanisms are summarized in Figure 5.

water from the cell into large sinks at the vascular endfeet to help regulate cell volume. This prediction is supported by the polarized distribution of Kir4.1 and AQP4 at the perivascular astrocyte endfeet, providing a convenient route to relieve excessive intracellular K^+ and water burden. With improved imaging capability, future studies may be able to detect more localized changes in astrocyte process volume associated with transient fluxes in K^+.

3.4 | NKCC and KCC

Shifts in extra- or intracellular ion concentrations are known to have profound effects on the electrical repulsion and driving forces that manipulate ion movement across the plasma membrane. Simultaneously it is known that changes in the osmotic gradient can trigger water movement, independent of the electrical forces governing the movement of ions. Co-transporters NKCC1 (sodium-potassium-chloride cotransporter type 1) and KCC (potassium-chloride cotransporter) are responsible for facilitating the movement of ions across the membrane while maintaining electroneutrality. The net result of this transport can trigger a shift in the osmotic gradient, with implications on cell volume (Russell, 2000). Interestingly, the role of NKCC1 in potassium-induced astrocyte swelling may lie in its ability to transport water directly and in the direction of ion movement (Zeuthen, 2010). In an elegant series of experiments, Hamann et al. (2010) monitored the volume change of cultured epithelial cells expressing the co-transporter NKCC1. Using solutions of different ionic or osmotic composition, it became evident that a portion of water flux across the membrane was tied inextricably to movement of ions through NKCC1 (Hamann et al., 2010). This flux of water and ions was shown to be concomitant, suggesting permeability of NKCC1 to water itself. Importantly, through the use of an extracellular membrane-impermeable solute (mannitol), a fraction of water efflux occurred because of the increased osmotic gradient, while the remaining water influx followed the inward driving forces on Na^+ and Cl^-. Impressively, movement of water through NKCC1 directly

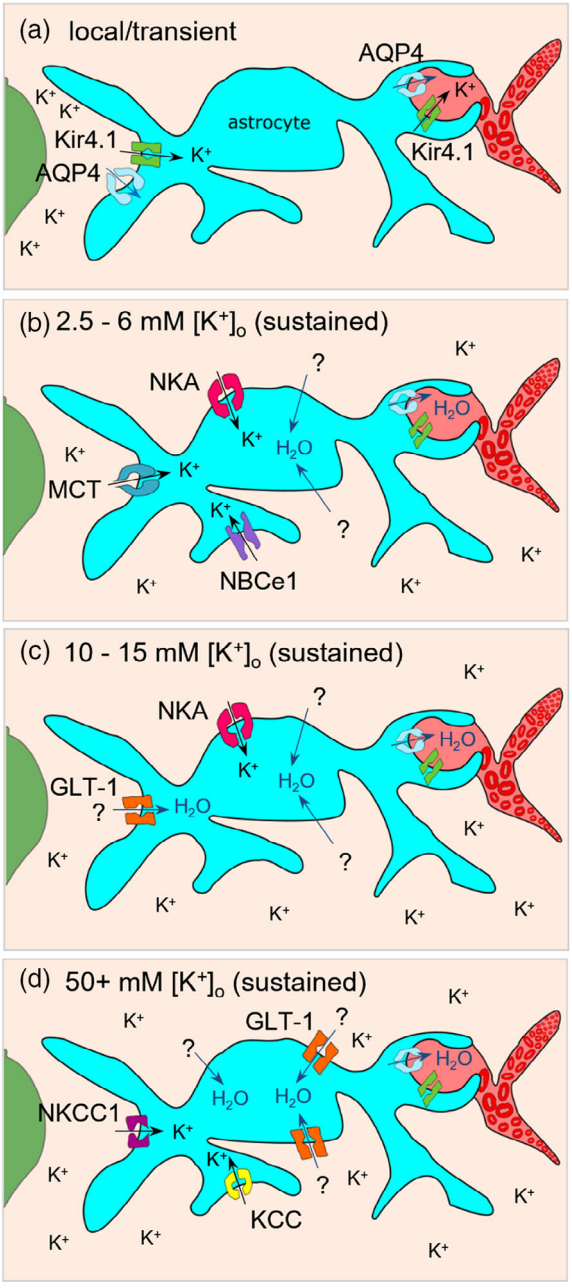

FIGURE 5 Summary of proposed mechanisms underlying astrocyte swelling and volume maintenance/recovery at different $[K^+]_o$. Conditions are shown along a range from: (a) Local/transient rises in $[K^+]_o$ near baseline levels through (d) pathological levels of $[K^+]_o$. (a) Transient elevations in $[K^+]_o$ due to local synaptic activity may enter astrocyte processes via Kirs along with water through AQP4 or other pathways (see text). K^+ and water is redistributed locally to areas of lower activity or siphoned via astrocyte endfeet into the vasculature on a very rapid timescale. (b) Increases in $[K^+]_o$ up to 5–6 mM by bath application or more sustained stimulation of neuronal afferents likely affects a larger area of the astrocyte domain resulting in more widespread and observable changes in astrocyte and ECS volume. Monocarboxylate transporters, NBCe1, and the Na^+/K^+ ATPase may all contribute to increased intracellular K^+ concentrations coupled to astrocyte volume increases in these conditions. With the inward ion movements under the auspices of transporters and pumps, the role of Kir4.1 and AQP4 is likely to ease intracellular K^+ and water burden through efflux to areas of lower activity or at endfeet into the vasculature. (c) At more moderate K^+ approaching ceiling levels during seizure or high frequency stimulation, the Na^+/K^+ ATPase plays a primary role in sequestering $[K^+]_o$ into astrocytes. (d) Strong cellular depolarization due to application of very high levels of $[K^+]_o$ (up to 100 mM) likely activates NKCC1 and reverses the direction of KCC, resulting in rapid ion influx and associated cell swelling. It is estimated that the astrocyte isoform of the Na^+/K^+ ATPase is effective at $[K^+]_o \leq \sim 12$ mM and therefore would be rapidly overwhelmed in these conditions. In (b), (c), and (d), data from several labs suggest that AQP4 is not required for water entry into astrocytes, which may instead occur by diffusing directly across the lipid bilayer, by passing through other dedicated water pore proteins such as the glucose or glutamate transporters, or in the case of (d), directly through NKCC/KCC co-transporters.

opposed the energetic force of the osmotic gradient, due to dependence on these ionic driving forces (Hamann et al., 2010). Further work in *Xenopus* oocytes using solutions of elevated potassium and/or urea confirmed that NKCC1 could ferry over 500 water molecules per protein turnover against a preexisting osmotic gradient (Zeuthen & Macaulay, 2012). Despite the capacity for NKCC1 in water movement, studies in various model systems suggest a contribution to cell swelling only in cases of very strong membrane depolarization at very high $[K^+]_o$.

Both NKCC1 and KCC have been studied in the scope of understanding mechanisms of regulatory volume increase (RVI) or decrease (RVD) in cultured astroglia and other cell types. Early experiments in primary astrocyte culture revealed that a portion of K^+ uptake could be inhibited with the use of the loop diuretics furosemide and bumetanide, which block NKCC1 and KCC (Kimelberg & Frangakis, 1985). Block of NKCC1/KCC prevented some of the astrocyte swelling normally triggered by the presence of hypotonic medium. Similarly in intact optic nerve, application of furosemide and bumetanide markedly depressed IOS signal normally corresponding to perfusion of elevated K^+ solution (MacVicar et al., 2002). In later studies, bumetanide block of NKCC1 in cultured astrocytes reduced potassium-induced swelling measured via DIC microscopy (MacVicar et al., 2002; Su et al., 2002 [Corrections added on June 16, 2022: Ritchie et al., 1981, has been changed to Su et al., 2002.]). Further experiments in astrocytes from NKCC1$^{-/-}$ mice clarified the need for NKCC1 activity to promote astrocyte swelling in elevated $[K^+]_o$ (Mironenko et al., 2021). However, it should be noted that this swelling occurred under extremely high potassium concentrations (75 mM K^+), far beyond the physiological limits for $[K^+]_o$ in the ECS of intact brain tissue.

While evidence for NKCC and KCC participation in swelling of cultured astroglia is apparent in conditions of strong membrane depolarization at very high $[K^+]_o$, their roles in more physiologically-relevant swelling models is less apparent. A more recent study found that NKCC1 did not play an obvious role in astrocyte K^+ buffering or astrocyte swelling in hippocampal slices post-stimulus (Larsen et al., 2014). Similarly with regard to KCC, its pharmacologic inhibition did not have any effect on ECS shrinkage in a stimulation-induced model of astrocyte swelling in hippocampal slices (Larsen & MacAulay, 2017). Recent work in hippocampal slices from young and old mice produced conflicting results regarding the role of NKCC1 in swelling. In younger mice, block of NKCC1 reduced soma swelling in astrocytes, while only in older mice (18 months) did the block lead to a reduction in swelling of the major processes (Kolenicova et al., 2020). Regardless of possible age-dependent changes in NKCC1 distribution and expression, astrocytes were exposed to 50 mM $[K^+]_o$ to induce swelling in these experiments, which is again far beyond physiological limits. In our recent study using 10.5 mM $[K^+]_o$ in hippocampal slices, application of the NKCC1-blocker bumetanide did not inhibit astrocyte swelling, suggesting that NKCC1 plays a relatively insignificant role in astrocyte swelling under more physiological concentrations of K^+ (Walch et al., 2020). Thus, our current perspective on the engagement of NKCC1 in the astrocyte swelling process may be heavily model dependent, as well as K^+ concentration specific.

3.5 | NBCe1

As has been discussed, movement of K^+ ions is directly coupled to water movement and cell swelling, but a potassium-rich ECS can also prime astrocytes for swelling independently of K^+ influx. With bouts of neuronal activity, $[K^+]_o$ increases result in astrocytic membrane depolarization (Anderson et al., 1995). Sodium bicarbonate cotransporter (NBCe1) activity is generated under these depolarized conditions, triggering an inward flux of sodium and bicarbonate ions (Ruminot et al., 2011). The resulting alkalization and pH increases serve as an important signal for glycolysis (Bittner et al., 2011). The major byproducts of astrocytic glycolysis include ATP, pyruvate and lactate. Importantly, lactate released from astrocytes can provide an energy source for active neurons (Brown & Ransom, 2007). The crucial role of NBCe1 in mediating increases in astrocytic glycolysis has been explored in detail by the Barros (Ruminot et al., 2011). Upon inhibition of NBCe1, K^+-induced depolarization in astrocytes fails to initiate intracellular alkalinization and thus glycolysis (Ruminot et al., 2011). More recently, the Barros group turned to experiments using NBCe1 knock-out mice, showing that only wild-type astrocytes rapidly metabolized glucose in response to 12 mM $[K^+]_o$, while NBCe1 KO astrocytes did not alter glucose metabolism (Ruminot et al., 2019). Subsequent experiments in NBCe1 KO brain slices showed that stimulation of Schaffer collaterals failed to bring about the intracellular alkalinization and glucose depletion that occurs in astrocytes with functional NBCe1 (Ruminot et al., 2019). When slices were stimulated in the presence of TTX, astrocyte levels of glucose, pyruvate and lactate remained unaltered, reaffirming the role of neuronal K^+ release in priming astrocytes for uptake of HCO_3^- and enter a glycolytic state (Ruminot et al., 2019).

Bicarbonate ion flux through NBCe1 may directly bring about astrocyte swelling. While imaging astrocytes in brain slices, a nearly 20% increase in soma area occurred after dual exposure to potassium and bicarbonate-containing ACSF over an extended time period (~40 min) (Florence et al., 2012). In the absence of HCO_3^-, potassium exposure over the time period yielded only a 5% increase in astrocyte soma area. Furthermore, this bicarbonate-mediated swelling could be reduced by nearly 10% with co-application of 4,4′-Diisothiocyano-2,2′-stilbenedisulfonic Acid (DIDS), an inhibitor of NBCe1 (Florence et al., 2012). Bicarbonate-independent volume changes occurred within the first 10 min of K^+ exposure, while bicarbonate-dependent volume increases occurred over approximately 30 min of dual potassium-bicarbonate exposure (Florence et al., 2012). These findings suggest a role for the NBCe1 in astrocyte swelling over prolonged or more sustained K^+ increases.

More recently, the MacAulay group stimulated brain slices to induce increases in $[K^+]_o$ and subsequent shrinkage of the ECS (Larsen & MacAulay, 2017). They found that with application of DIDS, approximately 25% of the ECS shrinkage could be inhibited, suggesting that NBCe1 plays a partial role in astrocyte swelling during stimulation-evoked increases in $[K^+]_o$ (Larsen & MacAulay, 2017). In our recent work, application of DIDS had no effect on direct astrocyte swelling measurements in 10.5 mM $[K^+]_o$ in acute hippocampal slices

(Walch et al., 2020). While these results suggested no role for NBCe1 in astrocyte swelling, it is worthwhile to note that K^+ was applied for only 5 min to assess acute effects on astrocyte volume. This brief time frame might be insufficient to engage NBCe1 swelling mechanisms as suggested by the findings of Florence et al. (2012). Furthermore, elevated K^+ was bath-applied, rather than released by tissue stimulation. Direct application of potassium may generate a different swelling response compared to stimulation of Schaffer collaterals, which will initiate a host of cellular responses (neurotransmitter release, ionotropic and metabotropic receptor activation, K^+ release, neurotransmitter reuptake, etc.). Overall, studies suggest that stimulation of neuronal afferents facilitates activity of NBCe1, which can lead to astrocyte volume increase. This NBCe1 swelling mechanism likely does not account for all of the astrocyte swelling induced by elevated $[K^+]_o$, given that multiple studies reported only modest reductions in swelling when NBCe1 was inhibited. However, any amount of ECS shrinkage might elevate extracellular glutamate concentration, and thus the activity of adjacent neurons.

3.6 | Monocarboxylate transporters (MCTs)

Lactate can be exchanged between astrocytes and neurons through MCTs in a process known as the "astrocyte-neuron lactate shuttle" (ANLS) (Mächler et al., 2016; Pellerin et al., 1998). Byproducts of glycolysis serve an important role in maintaining the ANLS, wherein astrocytes serve as lactate "sources" and neurons "sinks." Interactions between MCT and NBCe1 arise during shifts in intracellular pH. Elevations in extracellular $[K^+]_o$ depolarize astrocytes, activate NBCe1 and trigger inward fluxes of bicarbonate, alkalinizing the cell. In response, the rate of glycolysis and therefore the intracellular concentration of lactate, increases. MCTs provide an outlet for this lactate load, in the proximity of adjacent neurons. In culture, oocytes expressing NBCe1 and MCT experienced more lactate flux in comparison to oocytes expressing MCT alone, likely because the two channels cooperate in maintaining acid/base dynamics (Becker et al., 2004). Immunohistochemistry in mouse optic nerve showed MCT1 expression in astrocytes responsible for shuttling lactate and MCT2 on neurofilaments that actively uptake this energy source into neurons (Tekkok et al., 2005). In the same study, it was shown that in conditions without lactate or glucose, neurons encounter apparent energy failure and loss of action potentials. This implies the necessity of MCT function to support the ANLS, and the energetic needs of neurons.

Some evidence suggests a role for MCTs in astrocyte swelling responses. Early observations in bullfrog retinal epithelium indicated that a portion of water movement was tied to lactate permeability, such that water could be transported against osmotic gradients if coupled with lactate movement (Zeuthen et al., 1996). In the healthy rat brain slice, concurrent stimulation of the Schaffer collaterals and block of MCT with α-cyano-4-hydroxycinnamic acid (4-CIN) limited changes in the volume of the ECS (Larsen & MacAulay, 2017). Normally, stimulation brings about shrinkage of the ECS as the astrocytes swell, but 4-CIN co-application mitigated ~25% of this volume change, suggesting a role for MCT in astrocytic swelling. Most recently, co-expression of MCT and AQP9 channels has been investigated in retinal ganglion cells after optic nerve crush injury (Mori et al., 2020). AQP9 is expressed by astrocytes, is said to be water and lactate permeable, and thus may contribute to the volume changes of astrocytes that are actively participating in the ANLS. Collectively, these studies suggest that lactate movement may be a key driver of astrocytic volume changes. However, it remains unclear how export of lactate from astrocytes could be tied to water movement into the cell to promote swelling. Perhaps some of the volume changes ascribed to MCTs are driven by the synergistic activation of the NBCe1.

3.7 | Glutamate transporters

Under physiological conditions, ambient glutamate has been estimated to range anywhere from 2 nM–2 μM (Herman & Jahr, 2007). Nanomolar concentrations of glutamate tonically activate NMDARs (Cavelier & Attwell, 2005; Herman & Jahr, 2007), reinforcing the necessity of tight regulation of $[glutamate]_o$ in brain tissue. In astrocytes, excitatory amino acid transporters 1 (EAAT1) and 2 (rodent analogs GLAST and GLT-1, respectively) mediate uptake of glutamate from the ECS to balance tissue excitability and prevent excitotoxicity. In vivo inhibition of glutamate transporter synthesis in rats leads to elevated $[glutamate]_o$ and excitotoxicity, seen behaviorally as onset of paralysis (Rothstein et al., 1996). Thus, activity of glutamate transporters in response to neuronal excitatory synaptic transmission may mediate some of the volume changes in astrocytes.

In early work, direct application of glutamate to cultured C6 glioma cells triggered an increase in cell volume, which corresponded to an increase in glutamate uptake (Schneider et al., 1992). Similarly, glutamate application to Müller glia from rat ex vivo retinal tissue generated swelling (Izumi et al., 1999). This volume increase could be counteracted if glutamate was perfused in a sodium-free medium, suggesting involvement of the electrogenic glutamate transporters GLT-1 and GLAST in the swelling process (Izumi et al., 1999). In cultured rat astrocytes, cell swelling could also be triggered by application of a high-affinity glutamate transporter substrate called threo-beta-hydroxyaspartate (TBHA), even in the absence of glutamate itself (Koyama et al., 2000). By expressing GLT-1 in *Xenopus laevis* oocytes, the Zeuthen lab was able to simultaneously record glutamate currents through the transporter as volume change was assessed in individual cells (MacAulay, Gether, et al., 2001). They confirmed that: (1) glutamate uptake and cell swelling were positively correlated, (2) co-application of sodium and glutamate increased the water permeability of GLT-1, and (3) application of GLT-1 blocker DL-*threo*-β-benzyloxyaspartate (TBOA) reduced the water permeability (MacAulay et al., 2002). Molecular studies of GLT-1 mutants revealed important conformational changes upon glutamate binding that accommodated water molecules (Vandenberg et al., 2011), and glutamate transporters possess passive water permeability in addition to water movement coupled to glutamate uptake (MacAulay & Zeuthen, 2010). While the water permeability of GLT-1 is not so much

in question, whether these transporters are responsible for substantial water movement into astrocytes during neuronal activity remains unclear. In elevated K^+ conditions in acute hippocampal slices that cause substantial neuronal firing, astrocyte swelling profiles were identical in the presence of TTX (Walch et al., 2020), arguing against a role for activity-dependent glutamate uptake in significant astrocyte swelling responses over acute time scales. However, the passive water permeability of glutamate transporters may play a role in water movement, discussed in more detail below.

3.8 | The Na^+/K^+ ATPase (NKA)

The NKA performs a critical function necessary for cell survival, namely the maintenance of the sodium and potassium ionic gradients across the plasma membrane. Physiological processes like the firing of action potentials or sodium-dependent glutamate uptake by astrocytes rely on the NKA to sustain the Na^+ and K^+ gradients as well as the resting membrane potential critical for ionic driving forces. Inhibition of the pump by oxygen–glucose deprivation (OGD), ouabain, or barium chloride can lead to neuronal swelling, dendritic beading, and severe health consequences for cells and brain tissue over time (Douglas et al., 2011; Larsen et al., 2014; Risher et al., 2009; Walz et al., 1984). Early work established that the astrocytic NKA is quickly activated by small increases in $[K^+]_o$ and therefore played a primary role in potassium uptake by astrocytes (Kimelberg et al., 1995; Ransom et al., 2000; Walz et al., 1984; Walz & Hinks, 1985, 1986). Walz and coworkers found that K^+ uptake via the NKA was fast, occurring almost without delay, in response to modest increases of $[K^+]_o$ to 12 mM in astrocyte culture (Walz & Hertz, 1983; Walz & Hinks, 1986). Inhibition of cotransporters with furosemide also reduced K^+ influx into astrocytes to a similar degree as ouabain, but these effects were not additive, and K^+ channels only appeared to play a role when both the NKA and cotransport were blocked (Walz & Hinks, 1986). These findings led to the assumption that astrocytes express a unique isoform of the NKA that is sensitive to increases in K^+ in the physiological range, as opposed to the neuronal isoform which is insensitive to changes in $[K^+]_o$, but rather responds to changes in $[Na^+]_i$ (Ballanyi et al., 1987; Ransom et al., 2000; Rose & Ransom, 1996). More recent studies of NKA molecular structure have confirmed this hypothesis. Astrocytic NKA are predominantly of the $\alpha 2\beta 2$ isoform, which is far more sensitive to extracellular potassium increases compared to the main $\alpha 1\beta 1$, $\alpha 3\beta 1$ NKA isoforms expressed by neurons (Melone et al., 2019; Stoica et al., 2017).

In brain slice work, Larsen et al. (2014) found that block of NKA did not affect ECS volume changes induced by stimulation of Schaffer collaterals, in contrast to the evident role the NKA plays in sequestering potassium. Later work from the MacAulay group suggested that while NKA is responsible for potassium uptake, the NBCe1 and MCT transporters may actually participate more in the water shifts (Larsen & MacAulay, 2017). In contrast, it was recently observed that ~75% of acute K^+-induced astrocyte swelling could be blocked by 50 μM ouabain, implicating the NKA (Walch et al., 2020). The remaining ~25% of astrocyte swelling remained unaccounted for, suggesting possible involvement of other mechanisms. However, block of NBCe1, MCT (indirectly by DIDS), NKCC1/KCC and Kir4.1 failed to reduce any amount of astrocyte swelling (Walch et al., 2020). The incomplete block of astrocyte swelling by 50 μM ouabain could be explained in part by ouabain-potassium competition. Because K^+ and ouabain compete for the same sites, elevated $[K^+]_o$ can replace ouabain and attenuate the inhibitory effect of ouabain (Walz & Hinks, 1986). Further experiments using higher ouabain concentrations and/or lower $[K^+]_o$ could test this possibility. Overall, the findings of Walch et al. (2020) suggested that the astrocyte NKA plays a predominant role in astrocyte swelling responses in moderately elevated $[K^+]_o$ conditions, in line with its role in K^+ clearance. It is worth reiterating the possible differences that could arise from use of different experimental approaches. In Walch et al. (2020), volume measurements of astrocytes were assessed during a 5 min bath application of K^+. Stimulus-generated potassium increases might instead engage more local K^+ buffering pathways and limit involvement of the NKA until those pathways become saturated. In support of more than one mechanism, computational modeling of potassium uptake in conjunction with ECS shrinkage (from astrocyte swelling) suggested that the NKA itself could not account for all of the volume change occurring in astrocytes under conditions of elevated potassium (Murakami & Kurachi, 2016; Ostby et al., 2009). Interestingly, these models predicted different scenarios depending on the locality of other transporters and ion channels, the built-in conformity (or lack thereof) of the ECS, and the participation of neurons. For example, the locality of Kir4.1 channels regionally affected potassium buffering such that the role NKA plays is locally modulated (Murakami & Kurachi, 2016). In brain slice experiments, stimulation-induced increases in local potassium led to the finding that Kir4.1 channels play a small role in *local* potassium buffering, while block of NKA inhibited a large portion of post-stimulus potassium uptake (Larsen et al., 2014). Therefore, mechanisms of astrocyte potassium clearance and volume change are likely dependent on the subcellular localization of the pumps, channels and transporters, as well as the region exposed to potassium itself. The many experimental conditions and approaches which have been used to measure astrocyte swelling have been taken into account in the model summary of swelling mechanisms in elevated $[K^+]_o$ presented in Figure 5.

4 | THE NKA AND WATER MOVEMENT: HOW DOES PUMP ACTIVITY LEAD TO ASTROCYTE SWELLING?

Recent studies using MRI indicate that there is considerable water movement tied to NKA activity (Bai et al., 2018; Springer Jr., 2018). However, how NKA activity leads to astrocyte swelling is not readily apparent. The pump moves 3 Na^+ out for every 2 K^+ in each cycle, resulting in a net loss of ions from the cell and an outward osmotic gradient. Presumably, water would follow this outward gradient,

resulting in cellular shrinking. How the pump activity leads to astrocyte swelling is further confounded by the observation that inhibition of the pump by ouabain or OGD can lead to swelling of neurons and glia. These observations suggest that there must be other processes working hand-in-hand with the NKA to produce a net increase in intracellular osmolarity *in conditions of elevated potassium*. This possibility is supported by the following: First, despite the known pump stoichiometry, Walz and colleagues found that the intra-astrocytic K^+ gain in response to 12 mM $[K^+]_o$ exceeds the concomitant Na^+ loss by far (Walz & Hinks, 1985). The decrease in $[Na^+]_i$ corresponded to only about 10% of the accumulated $[K^+]_i$ (Walz & Hertz, 1983). This is likely because inward movement of Na^+ through other membrane transport processes is tightly coupled to pump activity - otherwise the pump would rapidly become ineffective at K^+ removal as intracellular Na^+ falls (Larsen et al., 2016; Rose & Ransom, 1996; Walz & Hertz, 1983). Maintenance of intracellular Na^+ plus rapid accumulation of $[K^+]_i$ could provide the bulk of the increase in intracellular osmolarity needed for water to move into the cell. Electroneutrality could be maintained by a combination of some influx of chloride (although it has been shown by Walz and colleagues that intracellular Cl^- levels do not rise very much with modest increases in $[K^+]_o$), reduced *efflux* of chloride due to the K^+-induced membrane depolarization, and production of endogenous anionic metabolites, such as bicarbonate and lactate (Ritchie, Packey, et al., 1981; Walz & Hertz, 1983). As to the latter point, many cellular activities are tied to the NKA, in particular cellular metabolism. Thus, increased cycling of the astrocytic NKA by a sudden increase in $[K^+]_o$ will be coupled to increased glucose transport activity, oxygen demand, and generation of pyruvate, lactate, bicarbonate, and ATP through glycolysis and oxidative metabolism. In summary, increased $[K^+]_o$ may lead to astrocyte swelling through significant pump-driven K^+ accumulation, maintenance of $[Na^+]_i$ to maintain pump efficiency, increased production of cellular metabolites and endogenous anions, and retention of Cl^- due to membrane depolarization.

5 | HOW DOES WATER ENTER THE ASTROCYTE?

There are two possible routes for water to permeate into astrocytes, leading to swelling. The first is through transmembrane proteins that form a water pore or channel, and the second is diffusion directly across the lipid bilayer. In either case, water will follow the movement of ions or solutes, either together with the ions themselves without need of a pre-existing osmotic gradient, or in the direction of an established gradient. As to a protein pore route, there are many possibilities. Almost all channel proteins are capable of passing water; this is called the streaming potential (Alcayaga et al., 1989; Horner et al., 2018; Horner & Pohl, 2018; Pohl, 2004; Rosenberg & Finkelstein, 1978). Even the highly specific K^+ channels in which individual K^+ ions are stripped of water as an essential step in permeation are thought to pass water in a single file stream between ions in a "soft knock-on" model (Mironenko et al., 2021). However, it has been generally considered that expression levels of ion channel proteins and channel open times are insufficient to permit physiologically significant amounts of water movement (Haines, 1994). Transporters provide another potential route for water. Glucose transporters, which would be stimulated by increased metabolic demand, are water permeable (Erokhova et al., 2016; Fischbarg et al., 1990; Iserovich et al., 2002; Loike et al., 1996; MacAulay, Bendahan, et al., 2001). For astrocytes specifically, dedicated studies in Xenopus oocytes and epithelial cells in vitro have identified several candidate water permeable cotransporters expressed by astrocytes including NKCC, KCC and glutamate transporters (MacAulay, Gether, et al., 2001; Zeuthen & MacAulay, 2002, 2012; Zhou et al., 2020). However, as detailed above, several recent studies in intact brain tissue have provided compelling evidence that NKCC, KCC and activity-dependent glutamate uptake are not involved in ECS constriction or real-time astrocyte volume increases associated with mild- to moderate elevations in extracellular K^+. Of course, AQP4 was also regarded as a key passive water pathway for astrocytes responsible for astrocyte swelling in hypoosmolar and high K^+ conditions, and also provided as an explanation for an inability to quantify such changes in neurons (Andrew et al., 2007; Risher et al., 2009). This assertion has now been challenged on many levels, and it is now clear that there is more to it than this simple explanation. Numerous studies using $AQP4^{-/-}$ mice and a variety of techniques to measure cell swelling have shown that not only is AQP4 not required for astrocyte swelling in hypoosmolar (Murphy, Davila, et al., 2017) or elevated K^+ conditions (Walch et al., 2020), but further, that a key role for AQP4 (and Kir4.1) may be to *extrude* water (and K^+) from the cell for efficient K^+ siphoning and to assist in cellular volume maintenance or recovery.

Channel, transporter, or pore-mediated pathways may not be necessary for significant and rapid water movement across cell membranes. In most mammalian cells, plasma membranes have high water permeability, as water can diffuse relatively rapidly across the lipid bilayer (Haines, 1994; Hannesschlaeger et al., 2019; Przybylo et al., 2021). Aquaporin expression is thought to be rate-limiting for fast water transport in a few, relatively water-impermeant cells such as epithelia (reviewed in Kimelberg, 2005). Application of hypoosmolar ACSF is especially noteworthy in this regard. When hACSF is applied, osmotic gradients are generated instantaneously for both neurons and astrocytes by dilution of extracellular solute concentration. No ion channels or transporters ever need to open to permit water to pass or to generate osmotic gradients for water movement. Furthermore, neurons, which are thought to lack functional water channels, readily swell in these conditions (Aitken et al., 1998), and swell to almost an identical amount and over a similar time course as astrocytes in intact brain tissue (Murphy, Davila, et al., 2017). This is further evidence that AQP4, which is not expressed by neurons, is not a requirement for water movement into cells. These findings also suggest that neurons and astrocytes may share a common water entry mechanism in many experimental conditions. It seems probable that this water entry mechanism is simple diffusion across the lipid bilayer.

This passive water movement can be fast, as significant volume increases occur in neurons and astrocytes within 1 min in hypo-osmolar conditions using standard solution perfusion rates (1–1.5 ml/min) (Lauderdale et al., 2015; Murphy, Davila, et al., 2017). Alternately, an undiscovered (or not yet tested) water permeability pathway expressed at similar levels by both neurons and astrocytes is responsible for their swelling in acute hypo-osmolar conditions.

In the case of rises in extracellular $[K^+]_o$, the water movement may also occur by simple diffusion across the lipid bilayer. A pore route to consider for water entry into astrocytes tied to elevated $[K^+]_o$ are the glutamate transporters. Although experiments have provided little evidence in support of activity-dependent co-transport of water through glutamate transporters as a mechanism contributing to astrocyte swelling in elevated $[K^+]_o$, the transporters also express a passive water entry pathway driven entirely by the osmotic gradient (reviewed in MacAulay and Zeuthen, 2010). Glutamate transporters are abundantly expressed by astrocytes and are located in the same membrane domains as the astrocytic Na^+/K^+ ATPase (Cholet et al., 2002; Melone et al., 2019), and thus provide a convenient route for passive water entry tied to elevated NKA activity (Figure 4). More work would be needed to identify mechanisms of water entry into astrocytes that leads to their swelling and associated consequences on brain tissue excitability.

5.1 | Looking ahead

As evidenced by the work above, the amount of conflicting results in this field of study is high. The mechanisms underlying rapid volume changes in astrocytes may be numerous, but poor ability to corroborate findings likely stems from differences in methodology, experimental conditions, model systems, and measurements. While many groups are moving into in vivo experiments involving volume imaging in intact rodent brain, popularity of image analysis programming has revealed differences in protocols. This lack of standardization is sure to introduce variability between findings within and between studies. The field's increased interest in studying astrocyte processes will likely continue the development of new tools such as SUSHI imaging to record and study volume changes and their mechanisms in localized intracellular domains, which may differ from those in the soma. With the advancement of new technologies that expand resolution of the astrocytic processes and endfeet, the field is poised to begin answering questions regarding the role of astrocyte processes in maintaining extracellular ion and neurotransmitter concentrations, local water movements and associated changes in the ECS, and regulating the exchange of water and other byproducts with the vasculature.

AUTHOR CONTRIBUTIONS

EW wrote early draft of the manuscript and designed the figures. TAF edited extensively and wrote sections on NKA induced swelling and water movements.

ACKNOWLEDGMENTS

We would like to thank the following funding agencies for their support of the work: NIH NINDS NS109918-01, NIH NIDA DA048815-01, and UCR Academic Senate.

CONFLICT OF INTEREST

The authors declare no potential conflict of interest.

DATA AVAILABILITY STATEMENT

Data sharing is not applicable to this article as no new data were created or analyzed in this study.

ORCID

Todd A. Fiacco https://orcid.org/0000-0003-1927-5349

REFERENCES

Aitken, P. G., Borgdorff, A. J., Juta, A. J., Kiehart, D. P., Somjen, G. G., & Wadman, W. J. (1998). Volume changes induced by osmotic stress in freshly isolated rat hippocampal neurons. *Pflügers Archiv*, *436*, 991–998.

Alcayaga, C., Cecchi, X., Alvarez, O., & Latorre, R. (1989). Streaming potential measurements in Ca2+-activated K+ channels from skeletal and smooth muscle. Coupling of ion and water fluxes. *Biophysical Journal*, *55*, 367–371.

Anderson, S., Brismar, T., & Hansson, E. (1995). Effect of external K+, Ca2+, and Ba2+ on membrane potential and ionic conductance in rat astrocytes. *Cellular and Molecular Neurobiology*, *15*, 439–450.

Andrew, R. D., Labron, M. W., Boehnke, S. E., Carnduff, L., & Kirov, S. A. (2007). Physiological evidence that pyramidal neurons lack functional water channels. *Cerebral Cortex*, *17*, 787–802.

Andrew, R. D., & MacVicar, B. A. (1994). Imaging cell volume changes and neuronal excitation in the hippocampal slice. *Neuroscience*, *62*, 371–383.

Arizono, M., Inavalli, V., Bancelin, S., Fernandez-Monreal, M., & Nagerl, U. V. (2021). Super-resolution shadow imaging reveals local remodeling of astrocytic microstructures and brain extracellular space after osmotic challenge. *Glia*, *69*, 1605–1613.

Badaut, J., Ashwal, S., Adami, A., Tone, B., Recker, R., Spagnoli, D., Ternon, B., & Obenaus, A. (2011). Brain water mobility decreases after astrocytic aquaporin-4 inhibition using RNA interference. *Journal of Cerebral Blood Flow and Metabolism*, *31*, 819–831.

Bai, R., Springer, C. S., Jr., Plenz, D., & Basser, P. J. (2018). Fast, Na(+) /K(+) pump driven, steady-state transcytolemmal water exchange in neuronal tissue: A study of rat brain cortical cultures. *Magnetic Resonance in Medicine*, *79*, 3207–3217.

Ballanyi, K., Grafe, P., & ten Bruggencate, G. (1987). Ion activities and potassium uptake mechanisms of glial cells in Guinea-pig olfactory cortex slices. *The Journal of Physiology*, *382*, 159–174.

Becker, H. M., Bröer, S., & Deitmer, J. W. (2004). Facilitated lactate transport by MCT1 when coexpressed with the sodium bicarbonate cotransporter (NBC) in Xenopus oocytes. *Biophysical Journal*, *86*, 235–247.

Benesova, J., Rusnakova, V., Honsa, P., Pivonkova, H., Dzamba, D., Kubista, M., & Anderova, M. (2012). Distinct expression/function of potassium and chloride channels contributes to the diverse volume regulation in cortical astrocytes of GFAP/EGFP mice. *PLoS One*, *7*, e29725.

Binder, D. K., Papadopoulos, M. C., Haggie, P. M., & Verkman, A. S. (2004). In vivo measurement of brain extracellular space diffusion by cortical surface photobleaching. *The Journal of Neuroscience*, *24*, 8049–8056.

Bittner, C. X., Valdebenito, R., Ruminot, I., Loaiza, A., Larenas, V., Sotelo-Hitschfeld, T., Moldenhauer, H., San Martín, A., Gutiérrez, R., Zambrano, M., & Barros, L. F. (2011). Fast and reversible stimulation of astrocytic glycolysis by K+ and a delayed and persistent effect of glutamate. *The Journal of Neuroscience*, *31*, 4709–4713.

Bosworth, A. P., & Allen, N. J. (2017). The diverse actions of astrocytes during synaptic development. *Current Opinion in Neurobiology*, *47*, 38–43.

Bourke, R. S., Kimelberg, H. K., Nelson, L. R., Barron, K. D., Auen, E. L., Popp, A. J., & Waldman, J. B. (1980). Biology of glial swelling in experimental brain edema. *Advances in Neurology*, *28*, 99–109.

Brown, A. M., & Ransom, B. R. (2007). Astrocyte glycogen and brain energy metabolism. *Glia*, *55*, 1263–1271.

Bugiani, M., Dubey, M., Breur, M., Postma, N. L., Dekker, M. P., Ter Braak, T., Boschert, U., Abbink, T. E. M., Mansvelder, H. D., Min, R., van Weering, J. R. T., & van der Knaap, M. S. (2017). Megalencephalic leukoencephalopathy with cysts: The *Glialcam*-null mouse model. *Annals of Clinical Translational Neurology*, *4*, 450–465.

Cavelier, P., & Attwell, D. (2005). Tonic release of glutamate by a DIDS-sensitive mechanism in rat hippocampal slices. *The Journal of Physiology*, *564*, 397–410.

Cholet, N., Pellerin, L., Magistretti, P. J., & Hamel, E. (2002). Similar perisynaptic glial localization for the Na+,K+-ATPase alpha 2 subunit and the glutamate transporters GLAST and GLT-1 in the rat somatosensory cortex. *Cerebral Cortex*, *12*, 515–525.

Chung, W. S., Allen, N. J., & Eroglu, C. (2015). Astrocytes control synapse formation, function, and elimination. *Cold Spring Harbor Perspectives in Biology*, *7*, a020370.

Chvatal, A., Anderova, M., Hock, M., Prajerova, I., Neprasova, H., Chvatal, V., Kirchhoff, F., & Sykova, E. (2007). Three-dimensional confocal morphometry reveals structural changes in astrocyte morphology in situ. *Journal of Neuroscience Research*, *85*, 260–271.

Dibaj, P., Kaiser, M., Hirrlinger, J., Kirchhoff, F., & Neusch, C. (2007). Kir4.1 channels regulate swelling of astroglial processes in experimental spinal cord edema. *Journal of Neurochemistry*, *103*, 2620–2628.

Dietzel, I., Heinemann, U., Hofmeier, G., & Lux, H. D. (1980). Transient changes in the size of the extracellular space in the sensorimotor cortex of cats in relation to stimulus-induced changes in potassium concentration. *Experimental Brain Research*, *40*, 432–439.

Douglas, H. A., Callaway, J. K., Sword, J., Kirov, S. A., & Andrew, R. D. (2011). Potent inhibition of anoxic depolarization by the sodium channel blocker dibucaine. *Journal of Neurophysiology*, *105*, 1482–1494.

Dudek, F. E., Obenaus, A., & Tasker, J. G. (1990). Osmolality-induced changes in extracellular volume alter epileptiform bursts independent of chemical synapses in the rat: Importance of non-synaptic mechanisms in hippocampal epileptogenesis. *Neuroscience Letters*, *120*, 267–270.

Erokhova, L., Horner, A., Ollinger, N., Siligan, C., & Pohl, P. (2016). The sodium glucose cotransporter SGLT1 is an extremely efficient facilitator of passive water transport. *The Journal of Biological Chemistry*, *291*, 9712–9720.

Fischbarg, J., Kuang, K. Y., Vera, J. C., Arant, S., Silverstein, S. C., Loike, J., & Rosen, O. M. (1990). Glucose transporters serve as water channels. *Proceedings of National Academy of Sciences of the United States of America*, *87*, 3244–3247.

Florence, C. M., Baillie, L. D., & Mulligan, S. J. (2012). Dynamic volume changes in astrocytes are an intrinsic phenomenon mediated by bicarbonate ion flux. *PLoS One*, *7*, e51124.

Genoud, C., Quairiaux, C., Steiner, P., Hirling, H., Welker, E., & Knott, G. W. (2006). Plasticity of astrocytic coverage and glutamate transporter expression in adult mouse cortex. *PLoS Biology*, *4*, e343.

Godin, A. G., Varela, J. A., Gao, Z., Danné, N., Dupuis, J. P., Lounis, B., Groc, L., & Cognet, L. (2017). Single-nanotube tracking reveals the nanoscale organization of the extracellular space in the live brain. *Nature Nanotechnology*, *12*(3), 238–243.

Gunnarson, E., Zelenina, M., Axehult, G., Song, Y., Bondar, A., Krieger, P., Brismar, H., Zelenin, S., & Aperia, A. (2008). Identification of a molecular target for glutamate regulation of astrocyte water permeability. *Glia*, *56*, 587–596.

Haines, T. H. (1994). Water transport across biological membranes. *FEBS Letters*, *346*, 115–122.

Haj-Yasein, N. N., Jensen, V., Østby, I., Omholt, S. W., Voipio, J., Kaila, K., Ottersen, O. P., Hvalby, Ø., & Nagelhus, E. A. (2012). Aquaporin-4 regulates extracellular space volume dynamics during high-frequency synaptic stimulation: A gene deletion study in mouse hippocampus. *Glia*, *60*, 867–874.

Haj-Yasein, N. N., Vindedal, G. F., Eilert-Olsen, M., Gundersen, G. A., Skare, O., Laake, P., Klungland, A., Thoren, A. E., Burkhardt, J. M., Ottersen, O. P., & Nagelhus, E. A. (2011). Glial-conditional deletion of aquaporin-4 (Aqp4) reduces blood-brain water uptake and confers barrier function on perivascular astrocyte endfeet. *Proceedings of the National Academy of Sciences of the United States of America*, *108*, 17815–17820.

Hamann, S., Herrera-Perez, J. J., Zeuthen, T., & Alvarez-Leefmans, F. J. (2010). Cotransport of water by the Na+-K+-2Cl(−) cotransporter NKCC1 in mammalian epithelial cells. *The Journal of Physiology*, *588*, 4089–4101.

Hamby, M. E., Coppola, G., Ao, Y., Geschwind, D. H., Khakh, B. S., & Sofroniew, M. V. (2012). Inflammatory mediators alter the astrocyte transcriptome and calcium signaling elicited by multiple G-protein-coupled receptors. *The Journal of Neuroscience*, *32*, 14489–14510.

Hannesschlaeger, C., Horner, A., & Pohl, P. (2019). Intrinsic membrane permeability to small molecules. *Chemical Reviews*, *119*, 5922–5953.

Hansson, E., Johansson, B. B., Westergren, I., & Ronnback, L. (1994). Mechanisms of glutamate induced swelling in astroglial cells. *Acta Neurochirurgica. Supplementum (Wien)*, *60*, 12–14.

Hatton, G. I., Perlmutter, L. S., Salm, A. K., & Tweedle, C. D. (1984). Dynamic neuronal-glial interactions in hypothalamus and pituitary: Implications for control of hormone synthesis and release. *Peptides*, *5*(Suppl 1), 121–138.

Henneberger, C., Bard, L., Panatier, A., Reynolds, J. P., Kopach, O., Medvedev, N. I., Minge, D., Herde, M. K., Anders, S., Kraev, I., Heller, J. P., Rama, S., Zheng, K., Jensen, T. P., Sanchez-Romero, I., Jackson, C. J., Janovjak, H., Ottersen, O. P., Nagelhus, E. A., … Rusakov, D. A. (2020). LTP induction boosts glutamate spillover by driving withdrawal of perisynaptic astroglia. *Neuron*, *108*, 919–936e911.

Herman, M. A., & Jahr, C. E. (2007). Extracellular glutamate concentration in hippocampal slice. *The Journal of Neuroscience*, *27*, 9736–9741.

Holthoff, K., & Witte, O. W. (1996). Intrinsic optical signals in rat neocortical slices measured with near-infrared dark-field microscopy reveal changes in extracellular space. *The Journal of Neuroscience*, *16*, 2740–2749.

Horner, A., & Pohl, P. (2018). Single-file transport of water through membrane channels. *Faraday Discussions*, *209*, 9–33.

Horner, A., Siligan, C., Cornean, A., & Pohl, P. (2018). Positively charged residues at the channel mouth boost single-file water flow. *Faraday Discussions*, *209*, 55–65.

Hrabetova, S., Hrabe, J., & Nicholson, C. (2003). Dead-space microdomains hinder extracellular diffusion in rat neocortex during ischemia. *The Journal of Neuroscience*, *23*, 8351–8359.

Inoue, H., & Okada, Y. (2007). Roles of volume-sensitive chloride channel in excitotoxic neuronal injury. *The Journal of Neuroscience*, *27*, 1445–1455.

Iserovich, P., Wang, D., Ma, L., Yang, H., Zuniga, F. A., Pascual, J. M., Kuang, K., De Vivo, D. C., & Fischbarg, J. (2002). Changes in glucose transport and water permeability resulting from the T310I pathogenic mutation in Glut1 are consistent with two transport channels per monomer. *The Journal of Biological Chemistry*, *277*, 30991–30997.

Izumi, Y., Kirby, C. O., Benz, A. M., Olney, J. W., & Zorumski, C. F. (1999). Muller cell swelling, glutamate uptake, and excitotoxic neurodegeneration in the isolated rat retina. *Glia*, *25*, 379–389.

Jentsch, T. J. (2016). VRACs and other ion channels and transporters in the regulation of cell volume and beyond. *Nature Reviews. Molecular Cell Biology*, *17*, 293–307.

Jessen, N. A., Munk, A. S., Lundgaard, I., & Nedergaard, M. (2015). The glymphatic system: A beginner's guide. *Neurochemical Research*, *40*, 2583–2599.

Kilb, W., Dierkes, P., Sykova, E., Vargova, L., & Luhmann, H. (2006). Hypoosmolar conditions reduce extracellular volume fraction and enhance epileptiform activity in the CA3 region of the immature rat hippocampus. *Journal of Neuroscience Research*, *84*, 119–129.

Kimelberg, H. K. (2005). Astrocytic swelling in cerebral ischemia as a possible cause of injury and target for therapy. *Glia*, *50*, 389–397.

Kimelberg, H. K., & Frangakis, M. V. (1985). Furosemide- and bumetanide-sensitive ion transport and volume control in primary astrocyte cultures from rat brain. *Brain Research*, *361*, 125–134.

Kimelberg, H. K., Rutledge, E., Goderie, S., & Charniga, C. (1995). Astrocytic swelling due to hypotonic or high K+ medium causes inhibition of glutamate and aspartate uptake and increases their release. *Journal of Cerebral Blood Flow and Metabolism*, *15*, 409–416.

Kitaura, H., Tsujita, M., Huber, V. J., Kakita, A., Shibuki, K., Sakimura, K., Kwee, I. L., & Nakada, T. (2009). Activity-dependent glial swelling is impaired in aquaporin-4 knockout mice. *Neuroscience Research*, *64*, 208–212.

Kletzien, R. F., Pariza, M. W., Becker, J. E., & Potter, V. R. (1975). A method using 3-O-methyl-D-glucose and phloretin for the determination of intracellular water space of cells in monolayer culture. *Analytical Biochemistry*, *68*, 537–544.

Kofuji, P., Ceelen, P., Zahs, K. R., Surbeck, L. W., Lester, H. A., & Newman, E. A. (2000). Genetic inactivation of an inwardly rectifying potassium channel (Kir4.1 subunit) in mice: Phenotypic impact in retina. *The Journal of Neuroscience*, *20*, 5733–5740.

Kolenicova, D., Tureckova, J., Pukajova, B., Harantova, L., Kriska, J., Kirdajova, D., Vorisek, I., Kamenicka, M., Valihrach, L., Androvic, P., Kubista, M., Vargova, L., & Anderova, M. (2020). High potassium exposure reveals the altered ability of astrocytes to regulate their volume in the aged hippocampus of GFAP/EGFP mice. *Neurobiology of Aging*, *86*, 162–181.

Koyama, Y., Ishibashi, T., Okamoto, T., Matsuda, T., Hashimoto, H., & Baba, A. (2000). Transient treatments with L-glutamate and threo-beta-hydroxyaspartate induce swelling of rat cultured astrocytes. *Neurochemistry International*, *36*, 167–173.

Larsen, B. R., Assentoft, M., Cotrina, M. L., Hua, S. Z., Nedergaard, M., Kaila, K., Voipio, J., & MacAulay, N. (2014). Contributions of the Na^+/K^+-ATPase, NKCC1, and Kir4.1 to hippocampal K^+ clearance and volume responses. *Glia*, *62*, 608–622.

Larsen, B. R., & MacAulay, N. (2017). Activity-dependent astrocyte swelling is mediated by pH-regulating mechanisms. *Glia*, *65*, 1668–1681.

Larsen, B. R., Stoica, A., & MacAulay, N. (2016). Managing brain extracellular K(+) during neuronal activity: The physiological role of the Na(+)/K(+)-ATPase subunit isoforms. *Frontiers in Physiology*, *7*, 141.

Lauderdale, K., Murphy, T., Tung, T., Davila, D., Binder, D. K., & Fiacco, T. A. (2015). Osmotic edema rapidly increases neuronal excitability through activation of NMDA receptor-dependent slow inward currents in juvenile and adult hippocampus. *ASN Neuro*, *7*, 175909141560511.

Lehre, K. P., & Rusakov, D. A. (2002). Asymmetry of glia near central synapses favors presynaptically directed glutamate escape. *Biophysical Journal*, *83*, 125–134.

Lichter-Konecki, U., Mangin, J., Gordish-Dressman, H., Hoffman, E., & Gallo, V. (2008). Gene expression profiling of astrocytes from hyperammonemic mice reveals altered pathways for water and potassium homeostasis in vivo. *Glia*, *56*, 365–377.

Loike, J. D., Hickman, S., Kuang, K., Xu, M., Cao, L., Vera, J. C., Silverstein, S. C., & Fischbarg, J. (1996). Sodium-glucose cotransporters display sodium- and phlorizin-dependent water permeability. *The American Journal of Physiology*, *271*, C1774–C1779.

Lundandersen, H., & Hertz, L. (1970). Effects of potassium and of glutamate on swelling and on sodium and potassium content in brain-cortex slices from adult rats. *Experimental Brain Research*, *11*, 199.

Lushnikova, I., Skibo, G., Muller, D., & Nikonenko, I. (2009). Synaptic potentiation induces increased glial coverage of excitatory synapses in CA1 hippocampus. *Hippocampus*, *19*, 753–762.

MacAulay, N., Bendahan, A., Loland, C. J., Zeuthen, T., Kanner, B. I., & Gether, U. (2001). Engineered Zn(2+) switches in the gamma-aminobutyric acid (GABA) transporter-1. Differential effects on GABA uptake and currents. *The Journal of Biological Chemistry*, *276*, 40476–40485.

MacAulay, N., Gether, U., Klaeke, D. A., & Zeuthen, T. (2002). Passive water and urea permeability of a human Na(+)-glutamate cotransporter expressed in Xenopus oocytes. *The Journal of Physiology*, *542*, 817–828.

MacAulay, N., Gether, U., Klaerke, D. A., & Zeuthen, T. (2001). Water transport by the human Na+-coupled glutamate cotransporter expressed in Xenopus oocytes. *The Journal of Physiology*, *530*, 367–378.

MacAulay, N., & Zeuthen, T. (2010). Water transport between CNS compartments: Contributions of aquaporins and cotransporters. *Neuroscience*, *168*, 941–956.

Mächler, P., Wyss, M. T., Elsayed, M., Stobart, J., Gutierrez, R., von Faber-Castell, A., Kaelin, V., Zuend, M., San Martín, A., Romero-Gómez, I., Baeza-Lehnert, F., Lengacher, S., Schneider, B. L., Aebischer, P., Magistretti, P. J., Barros, L. F., & Weber, B. (2016). In Vivo evidence for a lactate gradient from astrocytes to neurons. *Cell Metabolism*, *23*, 94–102.

MacVicar, B. A., Feighan, D., Brown, A., & Ransom, B. (2002). Intrinsic optical signals in the rat optic nerve: Role for K+ uptake via NKCC1 and swelling of astrocytes. *Glia*, *37*, 114–123.

Medina, D. C., Kirkland, D. M., Tavazoie, M. F., Springer, C. S., Jr., & Anderson, S. E. (2007). Na+/Ca2+-exchanger-mediated Mn2+-enhanced (1)H2O MRI in hypoxic, perfused rat myocardium. *Contrast Media & Molecular Imaging*, *2*, 248–257.

Meeks, J. P., & Mennerick, S. (2007). Astrocyte membrane responses and potassium accumulation during neuronal activity. *Hippocampus*, *17*, 1100–1108.

Melone, M., Ciriachi, C., Pietrobon, D., & Conti, F. (2019). Heterogeneity of astrocytic and neuronal GLT-1 at cortical excitatory synapses, as revealed by its colocalization with Na+/K+-ATPase alpha isoforms. *Cerebral Cortex*, *29*, 3331–3350.

Mironenko, A., Zachariae, U., de Groot, B. L., & Kopec, W. (2021). The persistent question of potassium channel permeation mechanisms. *Journal of Molecular Biology*, *433*, 167002.

Mori, S., Kurimoto, T., Miki, A., Maeda, H., Kusuhara, S., & Nakamura, M. (2020). Aqp9 gene deletion enhances retinal ganglion cell (RGC) death and dysfunction induced by optic nerve crush: Evidence that aquaporin 9 acts as an astrocyte-to-neuron lactate shuttle in concert with monocarboxylate transporters to support RGC function and survival. *Molecular Neurobiology*, *57*, 4530–4548.

Murakami, S., & Kurachi, Y. (2016). Mechanisms of astrocytic K(+) clearance and swelling under high extracellular K(+) concentrations. *The Journal of Physiological Sciences*, *66*, 127–142.

Murphy, T. R., Binder, D. K., & Fiacco, T. A. (2017). Turning down the volume: Astrocyte volume change in the generation and termination of epileptic seizures. *Neurobiology of Disease*, *104*, 24–32.

Murphy, T. R., Davila, D., Cuvelier, N., Young, L. R., Lauderdale, K., Binder, D. K., & Fiacco, T. A. (2017). Hippocampal and cortical pyramidal neurons swell in parallel with astrocytes during acute hypoosmolar stress. *Frontiers in Cellular Neuroscience*, *11*, 275.

Nase, G., Helm, P. J., Enger, R., & Ottersen, O. P. (2008). Water entry into astrocytes during brain edema formation. *Glia*, *56*, 895–902.

Newman, E. A. (1986). Regional specialization of the membrane of retinal glial cells and its importance to K+ spatial buffering. *Annals of the New York Academy of Sciences*, *481*, 273–286.

Newman, E. A., Frambach, D. A., & Odette, L. L. (1984). Control of extracellular potassium levels by retinal glial cell K+ siphoning. *Science*, *225*, 1174–1175.

Nicholson, C., & Hrabetova, S. (2017). Brain extracellular space: The final frontier of neuroscience. *Biophysical Journal*, *113*, 2133–2142.

Nicholson, C., Phillips, J. M., & Gardner-Medwin, A. R. (1979). Diffusion from an iontophoretic point source in the brain: Role of tortuosity and volume fraction. *Brain Research*, *169*, 580–584.

Nielsen, S., Nagelhus, E. A., AmiryMoghaddam, M., Bourque, C., Agre, P., & Ottersen, O. P. (1997). Specialized membrane domains for water transport in glial cells: High-resolution immunogold cytochemistry of aquaporin-4 in rat brain. *Journal of Neuroscience*, *17*, 171–180.

Ostby, I., Oyehaug, L., Einevoll, G. T., Nagelhus, E. A., Plahte, E., Zeuthen, T., Lloyd, C. M., Ottersen, O. P., & Omholt, S. W. (2009). Astrocytic mechanisms explaining neural-activity-induced shrinkage of extraneuronal space. *PLoS Computational Biology*, *5*, 5.

Pannicke, T., Iandiev, I., Uckermann, O., Biedermann, B., Kutzera, F., Wiedemann, P., Wolburg, H., Reichenbach, A., & Bringmann, A. (2004). A potassium channel-linked mechanism of glial cell swelling in the postischemic retina. *Molecular and Cellular Neurosciences*, *26*, 493–502.

Pellerin, L., Pellegri, G., Bittar, P. G., Charnay, Y., Bouras, C., Martin, J. L., Stella, N., & Magistretti, P. J. (1998). Evidence supporting the existence of an activity-dependent astrocyte-neuron lactate shuttle. *Developmental Neuroscience*, *20*, 291–299.

Pohl, P. (2004). Combined transport of water and ions through membrane channels. *Biological Chemistry*, *385*, 921–926.

Przybylo, M., Drabik, D., Doskocz, J., Iglic, A., & Langner, M. (2021). The effect of the osmotically active compound concentration difference on the passive water and proton fluxes across a lipid bilayer. *International Journal of Molecular Sciences*, *22*(20), 11099.

Ransom, B. R., Yamate, C. L., & Connors, B. W. (1985). Activity-dependent shrinkage of extracellular space in rat optic nerve: A developmental study. *The Journal of Neuroscience*, *5*, 532–535.

Ransom, C. B., Ransom, B. R., & Sontheimer, H. (2000). Activity-dependent extracellular K+ accumulation in rat optic nerve: The role of glial and axonal Na+ pumps. *The Journal of Physiology*, *522*(Pt 3), 427–442.

Risher, W. C., Andrew, R. D., & Kirov, S. A. (2009). Real-time passive volume responses of astrocytes to acute osmotic and ischemic stress in cortical slices and in vivo revealed by two-photon microscopy. *Glia*, *57*, 207–221.

Ritchie, T., Packey, D. J., Trachtenberg, M. C., & Haber, B. (1981). K+-induced ion and water movements in the frog spinal cord and filum terminale. *Experimental Neurology*, *71*, 356–369.

Rose, C. R., & Ransom, B. R. (1996). Intracellular sodium homeostasis in rat hippocampal astrocytes. *The Journal of Physiology*, *491*(Pt 2), 291–305.

Rosenberg, P. A., & Finkelstein, A. (1978). Interaction of ions and water in gramicidin A channels: Streaming potentials across lipid bilayer membranes. *The Journal of General Physiology*, *72*, 327–340.

Rothstein, J. D., Dykes-Hoberg, M., Pardo, C. A., Bristol, L. A., Jin, L., Kuncl, R. W., Kanai, Y., Hediger, M. A., Wang, Y., Schielke, J. P., & Welty, D. F. (1996). Knockout of glutamate transporters reveals a major role for astroglial transport in excitotoxicity and clearance of glutamate. *Neuron*, *16*, 675–686.

Ruminot, I., Gutiérrez, R., Peña-Münzenmayer, G., Añazco, C., Sotelo-Hitschfeld, T., Lerchundi, R., Niemeyer, M. I., Shull, G. E., & Barros, L. F. (2011). NBCe1 mediates the acute stimulation of astrocytic glycolysis by extracellular K+. *The Journal of Neuroscience*, *31*, 14264–14271.

Ruminot, I., Schmälzle, J., Leyton, B., Barros, L. F., & Deitmer, J. W. (2019). Tight coupling of astrocyte energy metabolism to synaptic activity revealed by genetically encoded FRET nanosensors in hippocampal tissue. *Journal of Cerebral Blood Flow and Metabolism*, *39*, 513–523.

Rungta, R. L., Choi, H. B., Tyson, J. R., Malik, A., Dissing-Olesen, L., Lin, P. J., Cain, S. M., Cullis, P. R., Snutch, T. P., & MacVicar, B. A. (2015). The cellular mechanisms of neuronal swelling underlying cytotoxic edema. *Cell*, *161*, 610–621.

Russell, J. M. (2000). Sodium-potassium-chloride cotransport. *Physiological Reviews*, *80*, 211–276.

Schneider, G. H., Baethmann, A., & Kempski, O. (1992). Mechanisms of glial swelling induced by glutamate. *Canadian Journal of Physiology and Pharmacology*, *70*(Suppl), S334–S343.

Shahar, E., Derchansky, M., & Carlen, P. (2009). The role of altered tissue osmolality on the characteristics and propagation of seizure activity in the intact isolated mouse hippocampus. *Clinical Neurophysiology*, *120*, 673–678.

Sofroniew, M. V. (2020). Astrocyte reactivity: Subtypes, states, and functions in CNS innate immunity. *Trends in Immunology*, *41*, 758–770.

Springer, C. S., Jr. (2018). Using (1)H2O MR to measure and map sodium pump activity in vivo. *Journal of Magnetic Resonance*, *291*, 110–126.

Steffensen, A. B., Sword, J., Croom, D., Kirov, S. A., & MacAulay, N. (2015). Chloride cotransporters as a molecular mechanism underlying spreading depolarization-induced dendritic beading. *The Journal of Neuroscience*, *35*, 12172–12187.

Stoica, A., Larsen, B. R., Assentoft, M., Holm, R., Holt, L. M., Vilhardt, F., Vilsen, B., Lykke-Hartmann, K., Olsen, M. L., & MacAulay, N. (2017). The α2β2 isoform combination dominates the astrocytic Na. *Glia*, *65*, 1777–1793.

Strohschein, S., Huttmann, K., Gabriel, S., Binder, D. K., Heinemann, U., & Steinhauser, C. (2011). Impact of aquaporin-4 channels on K+ buffering and gap junction coupling in the hippocampus. *Glia*, *59*, 973–980.

Su, G., Kintner, D. B., & Sun, D. D. (2002). Contribution of Na+−K+−Cl− cotransporter to high− K+ (o)-induced swelling and EAA release in astrocytes. *American Journal of Physiology-Cell Physiology*, *282*, C1136–C1146.

Sykova, E., & Nicholson, C. (2008). Diffusion in brain extracellular space. *Physiological Reviews*, *88*, 1277–1340.

Sykova, E., Vargova, L., Kubinova, S., Jendelova, P., & Chvatal, A. (2003). The relationship between changes in intrinsic optical signals and cell swelling in rat spinal cord slices. *NeuroImage*, *18*, 214–230.

Tekkok, S. B., Brown, A. M., Westenbroek, R., Pellerin, L., & Ransom, B. R. (2005). Transfer of glycogen-derived lactate from astrocytes to axons via specific monocarboxylate transporters supports mouse optic nerve activity. *Journal of Neuroscience Research*, *81*, 644–652.

Theodosis, D. T., Piet, R., Poulain, D. A., & Oliet, S. H. (2004). Neuronal, glial and synaptic remodeling in the adult hypothalamus: Functional consequences and role of cell surface and extracellular matrix adhesion molecules. *Neurochemistry International*, *45*, 491–501.

Toft-Bertelsen, T. L., Larsen, B. R., Christensen, S. K., Khandelia, H., Waagepetersen, H. S., & MacAulay, N. (2021). Clearance of activity-evoked K. *Glia*, *69*, 28–41.

Tonnesen, J., Inavalli, V., & Nagerl, U. V. (2018). Super-resolution imaging of the extracellular space in living brain tissue. *Cell*, *172*, 1108–1121e1115.

Traynelis, S. F., & Dingledine, R. (1988). Potassium-induced spontaneous electrographic seizures in the rat hippocampal slice. *Journal of Neurophysiology*, *59*, 259–276.

Traynelis, S. F., & Dingledine, R. (1989). Role of extracellular space in hyperosmotic suppression of potassium-induced electrographic seizures. *Journal of Neurophysiology*, *61*, 927–938.

Vandenberg, R. J., Handford, C. A., Campbell, E. M., Ryan, R. M., & Yool, A. J. (2011). Water and urea permeation pathways of the human excitatory amino acid transporter EAAT1. *The Biochemical Journal*, *439*, 333–340.

Ventura, R., & Harris, K. M. (1999). Three-dimensional relationships between hippocampal synapses and astrocytes. *The Journal of Neuroscience*, *19*, 6897–6906.

Walch, E., Murphy, T. R., Cuvelier, N., Aldoghmi, M., Morozova, C., Donohue, J., Young, G., Samant, A., Garcia, S., Alvarez, C., Bilas, A., Davila, D., Binder, D. K., & Fiacco, T. A. (2020). Astrocyte-selective volume increase in elevated extracellular potassium conditions is mediated by the Na. *ASN Neuro*, *12*, 1759091420967152.

Walz, W., & Hertz, L. (1983). Intracellular ion changes of astrocytes in response to extracellular potassium. *Journal of Neuroscience Research*, *10*, 411–423.

Walz, W., & Hinks, E. C. (1985). Carrier-mediated KCl accumulation accompanied by water movements is involved in the control of physiological K+ levels by astrocytes. *Brain Research*, *343*, 44–51.

Walz, W., & Hinks, E. C. (1986). A transmembrane sodium cycle in astrocytes. *Brain Research*, *368*, 226–232.

Walz, W., Shargool, M., & Hertz, L. (1984). Barium-induced inhibition of K+ transport mechanisms in cortical astrocytes–its possible contribution to the large Ba2+-evoked extracellular K+ signal in brain. *Neuroscience*, *13*, 945–949.

Watkins, S., & Sontheimer, H. (2012). Unique biology of gliomas: Challenges and opportunities. *Trends in Neurosciences*, *35*, 546–556.

Wetherington, J., Serrano, G., & Dingledine, R. (2008). Astrocytes in the epileptic brain. *Neuron*, *58*, 168–178.

Witcher, M. R., Kirov, S. A., & Harris, K. M. (2007). Plasticity of perisynaptic astroglia during synaptogenesis in the mature rat hippocampus. *Glia*, *55*, 13–23.

Wurm, A., Pannicke, T., Iandiev, I., Wiedemann, P., Reichenbach, A., & Bringmann, A. (2006). The developmental expression of K+ channels in retinal glial cells is associated with a decrease of osmotic cell swelling. *Glia*, *54*, 411–423.

Xie, L., Kang, H., Xu, Q., Chen, M. J., Liao, Y., Thiyagarajan, M., O'Donnell, J., Christensen, D. J., Nicholson, C., Iliff, J. J., Takano, T., Deane, R., & Nedergaard, M. (2013). Sleep drives metabolite clearance from the adult brain. *Science*, *342*, 373–377.

Yang, B. X., Zador, Z., & Verkman, A. S. (2008). Glial cell aquaporin-4 overexpression in transgenic mice accelerates cytotoxic brain swelling. *Journal of Biological Chemistry*, *283*, 15280–15286.

Yang, J., Vitery, M., Chen, J., Osei-Owusu, J., Chu, J., & Qiu, Z. (2019). Glutamate-releasing SWELL1 channel in astrocytes modulates synaptic transmission and promotes brain damage in stroke. *Neuron*, *102*, 813–827.e6.

Zelenina, M., & Brismar, H. (2000). Osmotic water permeability measurements using confocal laser scanning microscopy. *European Biophysics Journal*, *29*, 165–171.

Zeuthen, T. (2010). Water-transporting proteins. *The Journal of Membrane Biology*, *234*, 57–73.

Zeuthen, T., Hamann, S., & la Cour, M. (1996). Cotransport of H+, lactate and H2O by membrane proteins in retinal pigment epithelium of bullfrog. *The Journal of Physiology*, *497*(Pt 1), 3–17.

Zeuthen, T., & MacAulay, N. (2002). Cotransporters as molecular water pumps. *International Review of Cytology*, *215*, 259–284.

Zeuthen, T., & Macaulay, N. (2012). Cotransport of water by Na(+)-K(+)-2Cl(−) cotransporters expressed in Xenopus oocytes: NKCC1 versus NKCC2. *The Journal of Physiology*, *590*, 1139–1154.

Zhang, Y., Zhang, H., Feustel, P. J., & Kimelberg, H. K. (2008). DCPIB, a specific inhibitor of volume regulated anion channels (VRACs), reduces infarct size in MCAo and the release of glutamate in the ischemic cortical penumbra. *Experimental Neurology*, *210*, 514–520.

Zhou, J. J., Luo, Y., Chen, S. R., Shao, J. Y., Sah, R., & Pan, H. L. (2020). LRRC8A-dependent volume-regulated anion channels contribute to ischemia-induced brain injury and glutamatergic input to hippocampal neurons. *Experimental Neurology*, *332*, 113391.

Zhou, N., Gordon, G. R., Feighan, D., & MacVicar, B. A. (2010). Transient swelling, acidification, and mitochondrial depolarization occurs in neurons but not astrocytes during spreading depression. *Cerebral Cortex*, *20*, 2614–2624.

[Correction added on June 16, 2022, after first online publication: Ritchie et al. (1981) was deleted from the Reference section. Su et al. (2002) was added to the Reference section.]

How to cite this article: Walch, E., & Fiacco, T. A. (2022). Honey, I shrunk the extracellular space: Measurements and mechanisms of astrocyte swelling. *Glia*, *70*(11), 2013–2031. https://doi.org/10.1002/glia.24224